

Preparation of Hamming-Weight-Preserving Quantum States with Log-Depth Quantum Circuits

Yu Li^{1,2}, Guojing Tian^{*1,2}, Xiaoyu He^{†3}, and Xiaoming Sun^{‡1,2}

¹State Key Lab of Processors, Institute of Computing Technology, Chinese Academy of Sciences, Beijing 100190, China

²University of Chinese Academy of Sciences, Beijing 100049, China

³Huawei Taylor Lab, Shanghai, China

Abstract

Quantum state preparation is a critical task in quantum computing, particularly in fields such as quantum machine learning, Hamiltonian simulation, and quantum algorithm design. The depth of preparation circuit for the most general state has been optimized to approximately optimal, but the log-depth appears only when the number of ancillary qubits reaches exponential. Actually, few log-depth preparation algorithms assisted by polynomial ancillary qubits have been come up with even for a certain kind of non-uniform state. We focus on the Hamming-Weight-preserving states, defined as $|\psi_H\rangle = \sum_{\text{HW}(x)=k} \alpha_x |x\rangle$, which have leveraged their strength in quantum machine learning. Especially when $k = 2$, such Hamming-Weight-preserving states correspond to simple undirected graphs and will be called graph-structured states. Firstly, for the n -qubit general graph-structured states with m edges, we propose an algorithm to build the preparation circuit of $O(\log n)$ -depth with $O(m)$ ancillary qubits. Specifically for the n -qubit tree-structured and grid-structured states, the number of ancillary qubits in the corresponding preparation circuits can be optimized to zero. Next we move to the preparation for the HWP states with $k \geq 3$, and it can be solved in $O(\log \binom{n}{k})$ -depth using $O(\binom{n}{k})$ ancillary qubits, while the size keeps $O(\binom{n}{k})$. These depth and size complexities, for any $k \geq 2$, exactly coincide with the lower bounds of $\Omega(\log \binom{n}{k})$ -depth and $\Omega(\binom{n}{k})$ -size that we prove lastly, which confirms the near-optimal efficiency of our algorithms.

1 Introduction

Compared with classical algorithms, quantum computation has shown great superiority on a variety of computing tasks. Extensive efforts have been made by researchers to delve into the realm

^{*}tianguojing@ict.ac.cn

[†]This work does not belong to Huawei service achievement, and it is partially accomplished by Xiaoyu He in the Institute of Computing Technology, Chinese Academy of Science.

[‡]sunxiaoming@ict.ac.cn

of quantum machine learning [Cil+18; SSP15; Bia+17], Hamiltonian simulation [Ber+15; LC17; LC19], quantum network [Yan+18; Su+20], and graph algorithms [Dür+06; MSS07; SŠ21]. Many algorithms encounter an issue prior to their execution, which requires an initial quantum state to be specified. As a result, efficiently preparing a required quantum state becomes a fundamental task in quantum computing. This kind of problem is known as the Quantum State Preparation (QSP) problem.

The QSP problem can be rigorously defined as follows. Given a *unit* vector $\vec{\alpha} = (\alpha_0, \dots, \alpha_{2^n-1})^T \in \mathbb{C}^{2^n}$, the QSP problem requires designing a quantum circuit that outputs the state $|\psi_v\rangle = \sum_{x=0}^{2^n-1} \alpha_x |x\rangle$ when the input is $|0\rangle^{\otimes n}$, where $\{|0\rangle, |1\rangle, \dots, |2^n-1\rangle\}$ forms the computational basis of the n -qubit quantum system. For clarification, we may use binary strings in the following instead of decimal numbers to express the computational basis states. For example, $|6\rangle$ will be written as $|110\rangle$. Most of the previous studies on the QSP problem have focused on the preparation of general quantum states [Ber+05; PB11]. Sun *et al.* [Sun+23] provide a quantum circuit, which has a circuit size of $\Theta(2^n)$ and a circuit depth of $O(2^n/n)$ without ancillary qubits for preparing an arbitrary quantum state. When introducing $l \in O(2^n/(n \log n))$ ancillary qubits, the depth could be reduced to $\max\{O(n), O(\frac{2^n}{l+n})\}$. Yuan *et al.* [YZ23] give a circuit with depth $O(n + \frac{2^n}{l+n})$ for any given number of ancillary qubits, and this result has reached the depth lower bound of the general QSP problem for any number of ancillary qubits.

Although the above depth for general state preparation is approximately optimal, the preparation algorithm may not be efficient to any state. For example, only when the number of ancillary qubits l reaches exponential, the depth could be reduced to $O(n)$, the log of the number of non-trivial amplitudes in a general state. However, commonly used quantum states usually do not contain so many amplitudes states that the depth to prepare them should be optimized to log of the number of their non-trivial amplitudes, which is less than $O(n)$. The first popular states are sparse states, such as W-states [DVC00], GHZ-states [Gre+90], generalized Bell states [Cot+19], Bethe states [Van+21] and so on. Gleinig *et al.* [GH21] have given a quantum circuit for preparing sparse quantum states by using $O(nS)$ CNOT gates and $O(nS \log S)$ single-qubit gates, where S denotes the number of nonzero coefficients of \vec{v} . Li *et al.* [LL25] have built a quantum circuit with $O\left(\frac{nS}{\log(l+n)} + n\right)$ -size by using $l \in O(\frac{nS}{\log nS} + n)$ ancillary qubits. Luo *et al.* [LLL25] have presented a quantum circuit with $O\left(\frac{nS \log l}{l \log(l/n)} + \log nS\right)$ -depth and $O\left(\frac{nS}{\log(l/n)} + \frac{nS}{\log d}\right)$ -size by using $l \geq 6n$ ancillary qubits. Despite of these results, the depth is not yet to be optimized to log of the number of nontrivial basis states, i.e., $O(\log S)$.

Sparsity is a property of the amplitudes in a quantum state, except that, we turn to consider the structure of the basis states. Dicke states [Dic54] are states with special basis structures, and have been studied in different fields of quantum technology, such as quantum game theory [ÖSI07; FA02], and quantum networking [Pre+09]. A Dicke state is a state of the form $|D_k^n\rangle = \binom{n}{k}^{-1/2} \sum_{\text{HW}(x)=k} |x\rangle$, where $\text{HW}(x)$ denotes the Hamming Weight of x . For instance, $|D_2^4\rangle = \frac{1}{\sqrt{6}}(|0011\rangle + |0101\rangle + |1001\rangle + |0110\rangle + |1010\rangle + |1100\rangle)$. Bärtschi *et al.* [BE22] have constructed a quantum circuit for preparing Dicke states, which has a depth of $O(k \log(n/k))$ and uses $O(kn)$

CNOT gates. Yuan *et al.* [YZ25] improve the depth to $O(\log k \log(n/k) + k)$. Another kind of state with specific structure is the Cyclic state, which is in the form $|C_k^n\rangle = \frac{1}{\sqrt{n}} \sum_{\pi \in C(n)} \pi(|1\rangle^k |0\rangle^{n-k})$, where $C(n)$ is the cyclic permutation of the n binary digits. So $|C_k^n\rangle$ is the uniform superposition of computational basis that has k consecutive 1s in binary form, when treating the n digits as a cycle. For instance, $|C_3^5\rangle = \frac{1}{\sqrt{5}}(|00111\rangle + |01110\rangle + |11100\rangle + |11001\rangle + |10011\rangle)$. For Cyclic states, Mozafari *et al.* [MYD22] have presented a quantum circuit, which uses $O(n)$ CNOT gates.

Besides special basis structures, the amplitudes of Dicke states and Cyclic states are both uniform, which makes the depth of their preparation circuit low. The natural question is whether the circuit depth to prepare non-uniform states with such specific basis structures remains low. We will prove the depth can be optimized to the log of non-trivial amplitudes. We first define these states as Hamming-Weight-preserving (HWP) states, i.e.,

$$|\psi_H\rangle = \sum_{\text{HW}(x)=k} \alpha_x |x\rangle. \quad (1)$$

Without loss of generality, we can simply assume $k \leq n/2$. Actually, HWP states address two fundamental challenges in noisy intermediate-scale quantum (NISQ) systems: (1) the barren plateau problem in training variational quantum circuits, and (2) hardware limitations in scaling beyond 50+ qubits. By enforcing Hamming Weight conservation through hardware-efficient gates, these states enable exponential parameter compression while maintaining entanglement properties essential for quantum machine learning tasks [Mon+23].

Before explaining how to prepare the most general HWP states, we will focus on a special case of Hamming Weight (HW) $k = 2$, called graph-structured states¹. The preparation of graph-structured states is fundamental and will play an important role in that of HWP states with $k \geq 3$. Consider an undirected weighted graph $G = (V, E)$, where $V = \{v_1, v_2, \dots, v_n\}$ denotes the set of vertices, $w_{ij} \in \mathbb{R}_+$ ($\forall (v_i, v_j) \in E$) indicates the weight of the corresponding edge and the number of edges is $m = |E|$. In the following text, we use $v_i v_j$ to denote graph edges instead of the notation (v_i, v_j) . The graph-structured state is defined as

$$|\psi_G\rangle = \frac{1}{\sqrt{M}} \sum_{i < j, v_i v_j \in E} w_{ij} |e_i \oplus e_j\rangle, \quad (2)$$

where $M = \sum_{i < j, v_i v_j \in E} w_{ij}^2$ and $|e_i\rangle$ means the computational basis state that has a 1 on the i^{th} qubit and 0s on all other qubits. Here is an example, when the structure of G is shown in Figure 1, the corresponding graph-structured state $|\psi_G\rangle$ we aim to prepare is

$$\frac{1}{\sqrt{18}} \left(\sqrt{2} |1100000\rangle + \sqrt{3} |0110000\rangle + \sqrt{7} |0011000\rangle + \sqrt{3} |0100100\rangle + \sqrt{2} |0000110\rangle + \sqrt{1} |0000101\rangle \right). \quad (3)$$

¹It is worth mentioning that the concept of graph-structured states that we propose is different from the previously well-known concept of graph states [Cao+23]. We still decide to use “graph-structured states” because they can establish a very clear correspondence with graphs.

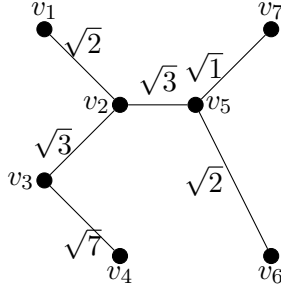


Figure 1: An undirected weighted graph whose corresponding quantum state is shown in Equation 3

In Equation 3, $\sqrt{18} = \sqrt{2 + 3 + 7 + 3 + 2 + 1}$ is the normalization coefficient, the computational base $\sqrt{2}|1100000\rangle$ has value 1 on the first and second place, which simply shows the edge v_1v_2 in G . The correspondence between other edges and computational basis is exactly the same as the former one. Obviously, the Dicke state with Hamming Weight of 2 corresponds to a complete graph, while the Cyclic state with $k = 2$ is similar to a cycle.

1.1 Main results

In this paper, we focus on how to prepare the graph-structured states and the HWP states in low depth. Our results include both upper and lower bounds. In the first place, we optimize the preparation of graph-structured states from three aspects corresponding to three common graphs: general graphs, trees, and grids. The preparation of general graph-structured quantum states can be solved in $O(\log n)$ -depth when using $O(m)$ ancillary qubits as shown in Theorem 1.

Theorem 1 *For an arbitrary graph G with n vertices, $|\psi_G\rangle$ can be prepared by a circuit with $O(\log n)$ -depth using $O(m)$ ancillary qubits.*

Then we will consider the optimization without ancillary qubits for graph-structured states. Fortunately, we find out that the tree-structured and grid-structured states can be prepared in $O(\log n)$ -depth without ancillary qubits, see Theorem 2 and Theorem 3 for details.

Theorem 2 *For an arbitrary tree G with n vertices, $|\psi_G\rangle$ can be prepared by a circuit with $O(\log n)$ -depth without ancillary qubits.*

Theorem 3 *For an arbitrary grid G with n vertices, $|\psi_G\rangle$ can be prepared by a circuit with $O(\log n)$ -depth without ancillary qubits.*

The graph-structured states discussed above are the states with a Hamming Weight of 2 in the computation basis. When the Hamming Weight is greater than 2, does the preparation circuit maintain the log-depth or not? The HWP states are certainly a kind of sparse states, the depths

of preparation circuits for sparse states have reached $O\left(\frac{nS \log l}{l \log(l/n)} + \log nS\right)$ when $l \geq 6n$ [LLL25], which is still greater than logarithm. Next we prove in Theorem 4 that the preparation of the HWP quantum states can be solved in $O(\log \binom{n}{k})$ -depth when using $O(\binom{n}{k})$ ancillary qubits.

Theorem 4 *For any HWP quantum state with parameters n and k , it can be prepared by a circuit with $O(\log \binom{n}{k})$ -depth using $O(\binom{n}{k})$ ancillary qubits.*

Finally, we prove the depth and size lower bounds of the HWP state preparation problem in Theorem 5, and the depth and size lower bounds of preparing the graph-structured states naturally follow in Theorem 6.

Theorem 5 *When using single- and double-qubit gates, almost all the HWP states with parameters n and k need to be prepared in $\Omega(\log \binom{n}{k})$ -depth and $\Omega(\binom{n}{k})$ -size, regardless of the number of ancillary qubits.*

Theorem 6 *When using single- and double-qubit gates, for almost all the graph G , the circuit for preparing $|\psi_G\rangle$ needs $\Omega(\log n)$ -depth and $\Omega(m)$ -size, regardless of the number of ancillary qubits.*

Combining the preparation algorithms and lower bound results together, we have discovered the HWP states can be prepared exactly by $\Theta(\log \binom{n}{k})$ -depth circuits with $O(\binom{n}{k})$ ancillary qubits, and the size still maintains $\Theta(\binom{n}{k})$, which implies our algorithms achieve approximate optimality both in depth and size complexities simultaneously. In other words, the HWP states are the currently only states, the preparation circuit depth of which can be optimized to logarithm with polynomial ancillary qubits. In order to better understanding our contributions, we summarize the related results in Table 1. In addition, we also analyze the classical computational complexity and find that the classical computational complexity of every algorithm is of the same order as the number of input parameters in the algorithm.

Table 1: Various quantum state preparation problems and complexity results.

Quantum State	Paper	# of ancillary qubits	# of CNOT	Depth	Notes
Arbitrary	[Sun+23]	0	$O(2^n)$	$O(\frac{2^n}{n})$	—
	[YZ23]	l	$O(2^n)$	$O(n + \frac{2^n}{l+n})$	—
Sparse	[GH21]	0	$O(nS)$	—	S is the number of non-zero coefficients.
	[MTS24]	2	$O(\frac{nS}{\log n} + n)$	—	
	[LL25]	$l \in O(\frac{nS}{\log nS} + n)$	$O(\frac{nS}{\log(l+n)} + n)$	—	
	[LLL25]	$l \geq 6n$	$O(\frac{nS}{\log(l/n)} + \frac{nS}{\log d})$	$O\left(\frac{nS \log l}{l \log(l/n)} + \log nS\right)$	
Dicke	[BE22]	0	$O(kn)$	$O(k \log \frac{n}{k})$	k is the Hamming Weight.
Dicke	[YZ25]	0	—	$O(\log k \log(n/k) + k)$	k is the Hamming Weight.
Cyclic	[MYD22]	0	$O(n)$	—	—
General graph-structured	This work	$O(m)$	$\Theta(m)$	$\Theta(\log n)$	m is the edge number of the graph.
Tree-structured	This work	0	$O(n)$	$O(\log n)$	—
Grid-structured	This work	0	$O(n)$	$O(\log n)$	—
HWP	This work	$O(\binom{n}{k})$	$\Theta(\binom{n}{k})$	$\Theta(\log \binom{n}{k})$	—

1.2 Proof techniques

For the preparation of Dicke states, Bärtschi *et al.* have presented a circuit construction for the Hamming Weight distribution block [BE22], based on which an optimized depth of $O(k \log(n/k))$ has been derived. One of the reasons why Dicke states can be prepared in low depth is that their coefficients are uniform. In fact, the uniform states are usually easier to prepare than the other states. The n -qubit uniform superposition state $1/\sqrt{2^n} \sum_{i=0}^{2^n-1} |i\rangle$ can be prepared by only 1-depth circuit (n -size), while the depth of the preparation circuit for the general superposition state $\sum_{i=0}^{2^n-1} \alpha_i |i\rangle$ reaches $O(2^n/n)$ without ancillary qubits ($\Theta(2^n)$ -size) [Sun+23]. The graph-structured states and HWP states we discuss in this paper are the superpositions of the same basis states with Dicke states, but the coefficients are arbitrary rather than uniform. This is exactly the difficult point. In the preparation algorithms for graph-structured states and HWP states, we solve it by various approaches below.

Prior to discussing specific methods, we introduce three key techniques applicable to both cases. First, chain-structured CNOT circuits admit log-depth implementations [Jia+20], as detailed in Section 2.2. Second, Section 2.3 establishes that both fan-in and fan-out gates can be synthesized via log-depth CNOT circuits. Third, the Unary Encoding [Joh+21] (see Section 3) enables log-depth preparation of arbitrary states in unary form. Notably, this encoding serves as the foundational step for nearly all our state preparation algorithms.

For the preparation of graph-structured states defined in Equation 2, we note that the Hamming weight of the basis state is equal to 2, thus the graph-structured states can be represented as corresponding planar graphs. There are some basic properties that can be employed to design the preparation algorithm. We first consider using ancillary qubits to prepare general graph-structured states in Section 4.1. This preparation algorithm, Algorithm 1, consists of three steps. The first step is the Unary Encoding, based on which we can generate all the coefficients (edge-weights) of the target graph-structured state in a unary encoded state storing in the ancillary qubits. Next, every ancillary qubit will be used as a controlled qubit to operate two CNOT gates on the two vertices of the corresponding edge. Finally, we need to restore the ancillary qubits, which will be realized by Toffoli gates controlled by the corresponding vertices. Actually, all the above three steps can be implemented by log-depth quantum circuits, which ensures the preparation of general graph-structured states keeps log-depth.

The upper algorithm using ancillary qubits seems easy, because the logarithmic-depth advantage fundamentally stems from the information dispersion facilitated by ancillary qubits. When there are no ancillary qubits, the absence of additional spaces forces us to focus on properties of different graphs and build more refined circuits. We introduce two more methods to improve the CNOT circuit depth in Section 5.1. For the preparation of tree-structured states, by choosing a vertex as the root vertex, the tree exhibits a rigorous hierarchical structure rooted in partial ordering and admits a natural bijective mapping between the vertex set (except root) and edge set. We can apply the Unary Encoding circuit and then a CNOT circuit directly on the working qubits. By optimizing the CNOT circuit using the method in Section 5.1, the CNOT circuit can be implemented in log-depth. For the preparation of grid-structured states, we use the divide-and-conquer algorithm. By

an $O(1)$ -depth circuit, the grid could be divided into two small grids, and the number of vertices in each small grid is less than $\frac{2}{3}n$. Finally, we face a graph consisting of independent edges, and this state could be prepared easily by applying a Unary Encoding circuit and a group of independent CNOT gates.

Although graph-structured states are also Hamming-Weight-preserving states, the Hamming Weight 2 is a constant, which has been considered as the factor of magnitude O . Thus, the above algorithm is not applicable to the preparation of general HWP states.

For the preparation of the HWP states defined in Equation 1, we first design a very similar algorithm, Lemma 13 according to Algorithm 1. Due to the increase in the number of controlled qubits, the size of this algorithm reaches $O(k \binom{n}{k})$, which exceeds the expected $O(\binom{n}{k})$. To achieve the optimal depth and size simultaneously, we consider to divide the basis state $|x\rangle$ into two parts, and prepare the two parts respectively. Based on Lemma 14, we derive the unique ordered pair (a, b) corresponding to an x such that $|x\rangle = |a\rangle|b\rangle$ and $x = 2^{n-i}a + b$, which enables us to decrease the number of controlled qubits. Algorithm 4 presents the detailed procedure to prepare $|\psi_H\rangle$. Besides the ancillary register A that is used to operate the Unary Encoding, there are six more ancillary registers, named B to F and q^* . After the Unary Encoding, we apply CNOT gates to generate $|e_a\rangle|e_b\rangle$ in register B , and record $|e_i\rangle$ in register D . Next we utilize Lemma 13 to generate $|x\rangle$ in register C , the size of which is much smaller than the original one. Then we use CNOT gates to derive $|x\rangle$ in working qubits controlled on the register C . As for restoring the register C , we should control on the working qubits and the register D , which means we apply a set of Toffoli gates. Now there are only register D left. It is noteworthy that the state in register D is unary codes, and we need to find out the different position is from the working qubits $|x\rangle$. We make $n - k + 1$ copies of $|x\rangle$, then apply the Hamming Weight Counter (HWC) to the copies and record the results to register E . If the result of the Hamming Weight, which is stored in register q^* , is 1, it can be used as controlled qubit to eliminate the state in register D . However, if the Hamming-Weight is bigger than 1, we need to make $n - k + 1$ copies of the state in register E similarly, and use HWC to the copies to determine if the HW is 1. The result will be recorded into register F , and the state in register D will be restored by controlled on register F and q^* .

Furthermore, we can also prove size and depth lower bounds for the preparation of HWP states in Section 8. The method is the common light cone and counting. In details, we compute the number of parameters which can be represented by the light cone and analyze the minimal number of parameters required to prepare general graph-structured states. Obviously, the former number should be greater than the latter, which will lead to the lower bounds of size and depth.

1.3 Discussion and open problems

While our construction establishes a depth-optimal quantum circuit for preparing HWP states using ancillary qubits, several fundamental questions remain:

- **Ancillary Qubit Minimization:** While maintaining $O(\binom{n}{k})$ -depth, can HWP states be prepared *with fewer ancillas or even without ancillas*? If impossible, what is the minimal ancilla count needed for log-depth preparation?

- **Non-Uniform State Preparation:** Do there exist other *practical* non-uniform quantum states that admit log-depth preparation circuits *with polynomially many ancillary qubits*?
- **Quantum Machine Learning Implications:** Given the significance of HWP states in QML, could our results imply hardness for quantum-classical learning separations?

The most compelling open challenge remains whether the ancilla requirement is *inherent* for depth-optimal preparation—resolving this would deepen our understanding of quantum complexity frontiers.

2 Preliminaries

We introduce some basic concepts and notations in quantum computation and graph theory in this section.

2.1 Elementary gates

Pauli gates and rotation gates about X-axis, Y-axis, and Z-axis are fundamental single-qubit gates in quantum computation. The CNOT gate is an elementary 2-qubit gate. The single-qubit gates, together with the CNOT gate, constitute the universal quantum gate, thus they are usually called the elementary quantum gates. In this article, when we talk about size complexity or depth complexity, we only consider circuits that consist of elementary quantum gates. We will frequently use the X gate, the H gate, the $C^2(R_y)$ gate and the $C^n(X)$ gate, where $C^2(X)$ is also known as the Toffoli gate. The matrix representations of X gate, $R_y(\theta)$ gate, H gate, and CNOT gate are as follows.

$$X = \begin{pmatrix} 0 & 1 \\ 1 & 0 \end{pmatrix}, R_y(\theta) = \begin{pmatrix} \cos \frac{\theta}{2} & -\sin \frac{\theta}{2} \\ \sin \frac{\theta}{2} & \cos \frac{\theta}{2} \end{pmatrix}, H = \frac{1}{\sqrt{2}} \begin{pmatrix} 1 & 1 \\ 1 & -1 \end{pmatrix}, \text{CNOT} = \begin{pmatrix} 1 & 0 & 0 & 0 \\ 0 & 1 & 0 & 0 \\ 0 & 0 & 0 & 1 \\ 0 & 0 & 1 & 0 \end{pmatrix}. \quad (4)$$

Actually, $C^2(R_y)$ gates and $C^2(X)$ gates can be implemented by using single-qubit gates and CNOT gates as shown in Figure 2.

$C^n(X)$ gates can also be decomposed into elementary gates.

Lemma 1 ([Gid]) *An $C^n(X)$ gate can be implemented by a quantum circuit of depth and size $O(n)$ with 1 ancillary qubits.*

Additionally, we give a simple way to calculate the depth and size complexity of any controlled gate, $C(U)$ when both the depth and size complexity of U are known.

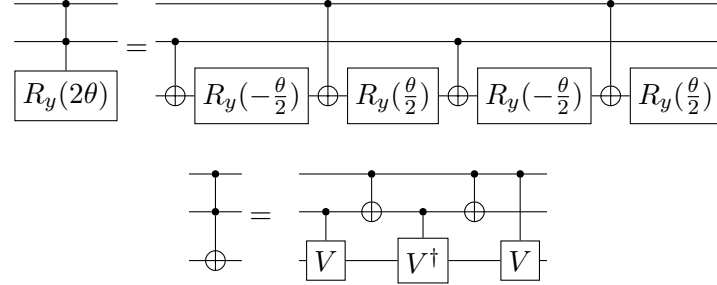


Figure 2: The decompositions of the $C^2(R_y(2\theta))$ gate and Toffoli gate, where $V = (1-i)(I+iX)/2$.

Lemma 2 *Assume U is an n -qubit quantum gate, the circuit implementing U has d depth and s size. When using $O(s)$ ancillary qubits, $C(U)$ can be implemented with $O(\log s + d)$ depth and $O(s)$ size.*

Proof. By making $O(s)$ copies of the control qubit, all the elementary gates in the circuit implemented U can get a unique control qubit, hence the elementary gates that are originally in the same layer can be applied simultaneously again. As Toffoli gates and controlled-single-qubit gates can be implemented with constant size, the overall depth, including the copying stage and the inverse stage, is $O(\log s + d)$, and the overall size is $O(s)$. \square

More basic concepts about quantum computation can be found in [NC10].

2.2 A chain-like CNOT circuit

It is well known that any n -qubit CNOT circuit can be viewed as an invertible linear map over \mathbb{F}_2^n , hence it can be represented by an invertible matrix in $\mathbb{F}_2^{n \times n}$.

A chain-like CNOT circuit means a sequence of CNOT gates applied on q_1, q_2, \dots, q_n , and the j^{th} CNOT gate is controlled by q_j and targets on q_{j+1} . Taking $n = 5$ as an example, its circuit and matrix representation are shown below

$$A = \begin{pmatrix} 1 & & & & \\ 1 & 1 & & & \\ 1 & 1 & 1 & & \\ 1 & 1 & 1 & 1 & \\ 1 & 1 & 1 & 1 & 1 \end{pmatrix}, A^{-1} = \begin{pmatrix} 1 & & & & \\ 1 & 1 & & & \\ 0 & 1 & 1 & & \\ 0 & 0 & 1 & 1 & \\ 0 & 0 & 0 & 1 & 1 \end{pmatrix}.$$

Figure 3: A chain-like CNOT circuit on 5 qubits and its matrix representation.

Lemma 3 ([Jia+20]) *The n -qubit chain-like CNOT circuit can be efficiently implemented by a CNOT circuit of $O(\log n)$ -depth without ancillary qubits.*

2.3 Fan-in and fan-out gate

A fan-in gate in quantum computation applies the following transformation.

$$\begin{aligned} |x_0\rangle|x_1x_2\cdots x_n\rangle &\rightarrow \left| \bigoplus_{j=0}^n x_j \right\rangle |x_1x_2\cdots x_n\rangle, \\ \forall (x_0, x_1, \dots, x_n) \in \mathbb{F}_2^{n+1}. \end{aligned} \tag{5}$$

On the other hand, a fan-out gate exchanges the role of all the qubits, compared to a fan-in gate. Specifically, a fan-out gate in quantum computation applies the following transformation.

$$\begin{aligned} |x_0\rangle|x_1x_2\cdots x_n\rangle &\rightarrow |x_0\rangle \otimes \left(\bigotimes_{j=1}^n |x_j \oplus x_0\rangle \right), \\ \forall \{x_0, x_1, \dots, x_n\} \in \mathbb{F}_2^{n+1}. \end{aligned} \tag{6}$$

Lemma 4 *The $(1+n)$ -qubit fan-in gate can be implemented by a CNOT circuit with $O(\log n)$ -depth without ancillary qubits.*

Proof. Suppose a fan-in gate with n control qubits can be applied in a depth of $f(n)$. Assume n is an even number (just for convenience). In the first layer of the circuit, we apply $n/2$ CNOT gates, each targeting on q_{2j-1} and controlled by $q_{2j}, j \in \{1, \dots, n/2\}$. Thus, the value of q_{2j-1} will become $x_{2j-1} \oplus x_{2j}$. If we continue applying a smaller fan-in gate on q_0 (as the target qubit) and $q_{2j-1}, j \in \{1, \dots, n/2\}$ (as the control qubits), the final value on q_0 will be $\bigoplus_{j=0}^n x_j$, which is exactly what we desired. Next, we add a final layer, which is the inverse of the first layer (actually, they are the same), so that all the $q_j, j \in \{1, \dots, n\}$ will be restored. Hence, we get $f(n) = 1 + f(\frac{n}{2}) + 1 = 2 + f(\frac{n}{2})$. This means $f(n) \in O(\log n)$. \square

The example of a $(1+8)$ -qubit fan-in gate is shown in Figure 4.

For the fan-out gate, note the equality in Figure 5. Therefore, by adding the H gates on each end of each qubit, the rest we need to do is just a fan-in gate (in fact, we have to add $2n$ H gates on q_0 , but two adjacent H gates will be eliminated as $H^2 = I$)

$$U_{\text{fan-out}} = H^{\otimes(n+1)} U_{\text{fan-in}} H^{\otimes(n+1)}. \tag{7}$$

Thus, the depth of a $(1+n)$ -qubit fan-out gate can also be implemented by a circuit with $O(\log n)$ -depth.

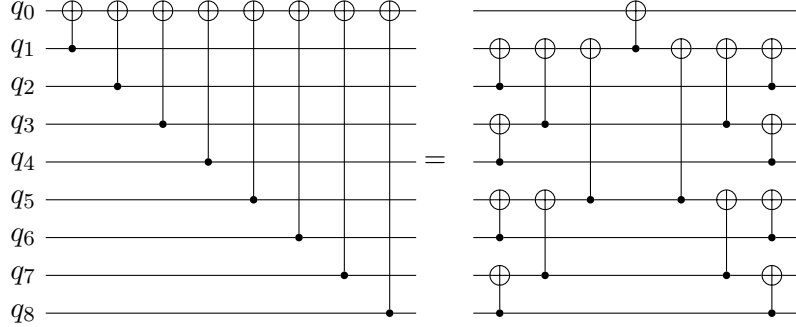


Figure 4: Two ways to implement a $(1 + 8)$ -qubit fan-in gate.

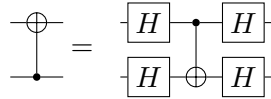


Figure 5: CNOT basis transformation.

2.4 Hamming Weight Counter

We introduce a new class of operators, which we refer to as Hamming Weight Counters, abbreviated as HWC gates.

Definition 1 For $n \in \mathbb{N}^*, k \in \mathbb{N}$ and $k \leq n$, a Hamming Weight Counter, HWC means an n -controlled quantum gate, the last qubit will be applied an X gate when the Hamming Weight of the first n qubit is exactly k . It is formally defined by its action on computational basis states:

$$HWC|x_1x_2 \cdots x_n\rangle |b\rangle = \begin{cases} |x_1x_2 \cdots x_n\rangle |b \oplus 1\rangle & \text{if } \sum_{i=1}^n x_i = k, \\ |x_1x_2 \cdots x_n\rangle |b\rangle & \text{otherwise.} \end{cases} \quad (8)$$

Eventually, an HWC gate checks if the Hamming Weight of the controlled qubits equals a required number and puts the result into the target qubit.

Lemma 5 ([ZNS25]) When using $O(n^2)$ ancillary qubits, an n -controlled HWC gate can be implemented with $O(\log n)$ -depth and $O(n^2)$ size.

2.5 Basic concepts in graph theory

In graph theory, a connected simple graph not containing any cycles is called a tree [Die24]. If we set a specific vertex (v_1 for example) as the root of the tree, then the height of a vertex (or node) means the distance between this vertex and v_1 , and the height of the tree means the maximum height of nodes in the tree. An $s \times t$ grid is a grid-like graph. The vertex set can be described as a point set in an xy-plane— $V = \{(a, b) | 0 \leq a \leq t-1, 0 \leq b \leq s-1\}$. Two vertices are adjacent iff

their Euclidean distance is 1. Therefore, a $s \times t$ grid is a graph with st vertices and $s(t-1) + t(s-1)$ edges.

3 Unary Encoding

In the rest of this article, we will frequently use a special kind of encoding, the Unary Encoding [Joh+21]. The Unary Encoding can prepare the state

$$\sum_{i=1}^l \alpha_i |e_i\rangle \quad (9)$$

for arbitrary $(\alpha_1, \alpha_2, \dots, \alpha_l)^T \in \mathbb{R}^l$ satisfying $\sum_{i=1}^l |\alpha_i|^2 = 1$.

Lemma 6 $\sum_{i=1}^l \alpha_i |e_i\rangle$ can be prepared by a quantum circuit with $O(\log l)$ -depth.

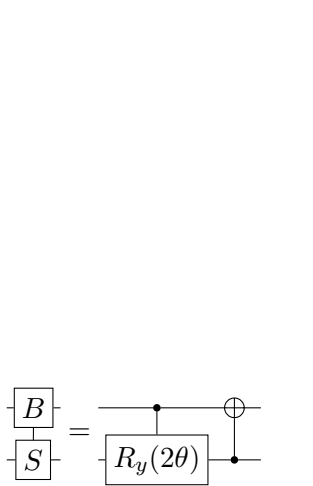
Proof. Here we briefly introduce the quantum gates used in the Unary Encoding. An $RBS(\theta)$ gate keeps the input $|00\rangle$ unchanged and turns the input $|10\rangle$ into $\cos \theta |10\rangle + \sin \theta |01\rangle$. Figure 6a is an available way to construct the $RBS(\theta)$ gate.

The main idea of the Unary Encoding is to split the coefficient into different parts in every layer. The parameter in every $RBS(\theta)$ gate is determined by the vector $\{\alpha_1, \alpha_2, \dots, \alpha_l\}$. We first apply a X gate on q_1 so that the state becomes $|e_1\rangle$. Note that at this moment, $|e_1\rangle$ is holding the whole coefficient. Then, we apply a $RBS(\theta)$ gate on q_1 and $q_{\lfloor l/2 \rfloor + 1}$, where θ is set as $\arccos \sqrt{\alpha_1^2 + \alpha_2^2 + \dots + \alpha_{\lfloor l/2 \rfloor}^2}$, and the state will become $\sqrt{\alpha_1^2 + \alpha_2^2 + \dots + \alpha_{\lfloor l/2 \rfloor}^2} |e_1\rangle + \sqrt{\alpha_{\lfloor l/2 \rfloor + 1}^2 + \dots + \alpha_l^2} |e_{\lfloor l/2 \rfloor + 1}\rangle$. Now, $|e_1\rangle$ is holding the whole coefficient of $|e_1\rangle, |e_2\rangle, \dots, |e_{\lfloor l/2 \rfloor}\rangle$, while $|e_{\lfloor l/2 \rfloor + 1}\rangle$ is holding the whole coefficient of $|e_{\lfloor l/2 \rfloor + 1}\rangle, \dots, |e_l\rangle$. So we can treat this $RBS(\theta)$ gate as splitting the coefficient into two parts. Each part is yet another Unary Encoding on half of the qubits, and the two parts can work in parallel. If we denote the depth of a l -qubit Unary Encoding as $f(l)$, we get $f(l) = O(1) + f(\frac{l}{2})$. Hence $f(l) \in O(\log l)$. \square

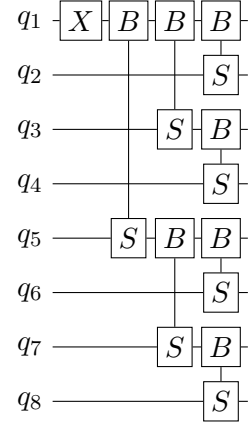
Taking $l = 8$ as an example, the Unary Encoding circuit is shown in Figure 6b. After the first $RBS(\theta)$ gate, the state becomes $\sqrt{\alpha_1^2 + \alpha_2^2 + \alpha_3^2 + \alpha_4^2} |e_1\rangle + \sqrt{\alpha_5^2 + \alpha_6^2 + \alpha_7^2 + \alpha_8^2} |e_5\rangle$, so that the later circuits on the top half and the bottom half can work at the same time.

4 Algorithm for preparing general graph-structured states with ancillary qubits

In this section, we will build the quantum circuit for the preparation of a general graph-structured quantum state with $O(m)$ ancillary qubits and $O(\log n)$ -depth.



(a) The decomposition of the $RBS(\theta)$ gate.



(b) The Unary Encoding on 8 qubits, where the parameters in every $RBS(\theta)$ gate are determined by the vector $(\alpha_1, \alpha_2, \dots, \alpha_8)^T$.

Figure 6: The Unary Encoding technique.

4.1 Preparation algorithm

We first introduce $l = m$ (recall that m is the number of edges, $m = |E|$) ancillary qubits $\{q'_1, q'_2, \dots, q'_m\}$, where each q'_j corresponds to the edge $e_j \in E$. Meanwhile, $|e'_j\rangle$ has the same meaning as $|e_j\rangle$, but we use it only to describe states on ancillary qubits. Denote the two vertices of the edge e_j as v_{j_1} and v_{j_2} . The detailed QSP procedure for a general graph-structured state is shown in Algorithm 1.

Lemma 7 *Algorithm 1 can correctly prepare the general graph-structured quantum state.*

Proof. By dividing the whole algorithm into 3 steps: line 1; line 2 to line 4; line 5 to line 7, we can easily check the state transformation after each step,

$$\begin{aligned}
 & |0\rangle^{\otimes n} \otimes |0\rangle^{\otimes m} \\
 \xrightarrow{1} & \frac{1}{\sqrt{M}} \sum_{e_j=v_{j_1}v_{j_2} \in E} w_{j_1j_2} |0\rangle^{\otimes n} \otimes |e'_j\rangle \\
 \xrightarrow{2 \text{ to } 4} & \frac{1}{\sqrt{M}} \sum_{e_j=v_{j_1}v_{j_2} \in E} w_{j_1j_2} |e_{j_1} \oplus e_{j_2}\rangle \otimes |e'_j\rangle \\
 \xrightarrow{5 \text{ to } 7} & \frac{1}{\sqrt{M}} \sum_{e_j=v_{j_1}v_{j_2} \in E} w_{j_1j_2} |e_{j_1} \oplus e_{j_2}\rangle \otimes |0\rangle^{\otimes n}.
 \end{aligned} \tag{10}$$

Thus, the algorithm is correct. \square

Algorithm 1 Preparation of a general graph-structured quantum state with $O(m)$ ancillary qubits.

Input: An arbitrary graph $G = (V, E)$, where $n = |V|$; n working qubits together with m ancillary qubits.

Output: The circuit that prepares $|\psi_G\rangle |0\rangle^{\otimes m}$.

- 1: Apply Unary Encoding on ancillary qubits, where the coefficient of $|e'_j\rangle$ is the weight of e_j divided by \sqrt{M} .
- 2: **for** every edge $e_j = v_{j_1}v_{j_2}$ **do**
- 3: Apply 2 CNOT gates both controlled by q'_j , and targeting on q_{j_1}, q_{j_2} respectively.
- 4: **end for**
- 5: **for** every edge $e_j = v_{j_1}v_{j_2}$ **do**
- 6: Apply a Toffoli gate controlled by q_{j_1} and q_{j_2} , targeting on q'_j .
- 7: **end for**
- 8: Return the whole circuit.

Theorem 7 (Restatement of Theorem 1) *Based on Algorithm 1, for an arbitrary graph G with n vertices, $|\psi_G\rangle$ can be prepared by a circuit with $O(\log n)$ -depth using $O(m)$ ancillary qubits.*

Proof. The first step of Algorithm 1 (line 1) is simply a Unary Encoding circuit on m ancillary qubits. Hence by Lemma 6, step 1 can be implemented in a depth of $O(\log m)$. As $m < \frac{n^2}{2}$, $O(\log m) = O(\log n)$.

For the second step (line 2 to 4), we will totally apply $2m$ CNOT gates. These gates are obviously commutable. We can divide the $2m$ CNOT gates into 2 sets, each with m CNOT gates. For $\forall j \in \{1, 2, \dots, m\}$, we put one CNOT gate controlled by q'_j into the first set, and put the other one into the second set. We can find that the CNOT gates in a single set can be treated as several independent fan-in gates. By Lemma 4, applying the CNOT gates in a single set can be implemented in a depth of $O(\log n)$. As there are only 2 sets, the $2m$ CNOT gates can be implemented in a depth of $O(\log n) + O(\log n) = O(\log n)$.

For the final step (line 5 to 7), we apply m Toffoli gates. Every $q'_j, j \in \{1, 2, 3, \dots, m\}$ will be used as target qubit exactly once, while some q_i will be used as control qubit for more than once, suppose t_i times. We can optimize the depth using the following method. We first apply a copying stage. We copy each q_i for $t_i - 1$ times (by adding t_i more ancillary qubits). Note that the number of ancillary qubits that are newly added in this step is $\sum_{i=1}^n (t_i - 1) = 2m - n = O(m)$, and the copying stage has a depth of $\log(\max_i t_i) = O(\log n)$. Secondly, we apply m Toffoli gates by using q_i or its copy as control qubits. As all Toffoli gates run independently, the depth of this stage is just the depth of one Toffoli gate, which is a constant. Finally, we apply the inverse operation of the copying stage. Thus, the final step can be implemented in a depth of $O(\log n) + O(\log n) = O(\log n)$.

Combining all three steps together, we can get that $|\psi_G\rangle$ can be generated in a depth of $O(\log n)$, when using $O(m)$ ancillary qubits. \square

For better understanding of Algorithm 1, we provide an example. The input graph G is shown in Figure 7, where the weights can be set to arbitrary value. That is, our goal is to prepare the state

$|\psi_G\rangle = w_{14} |10010\rangle + w_{15} |10001\rangle + w_{23} |01100\rangle + w_{24} |01010\rangle + w_{25} |01001\rangle + w_{34} |00110\rangle + w_{35} |00101\rangle$. The output is the QSP circuit for $|\psi_G\rangle$ in Figure 8. For the first step (line 1), we apply the Unary Encoding circuit, the parameters in all RBS gates depend on the arbitrary weights $w_{v_i v_j}$ ($v_i v_j \in E$). For the second step (line 2 to 4) we apply $2 \times 7 = 14$ CNOT gates, and these CNOT gates can be divided into two parts (denoted as green color and red color). CNOT gates in the same color belong to the same part, and can be applied in $O(\log 7)$ -depth. For the final step (line 5 to 7), we apply 7 Toffoli gates. We have completed the preparation of $|\psi_G\rangle$.

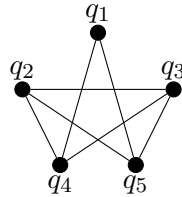


Figure 7: The input graph G , where the weights can be set to arbitrary value.

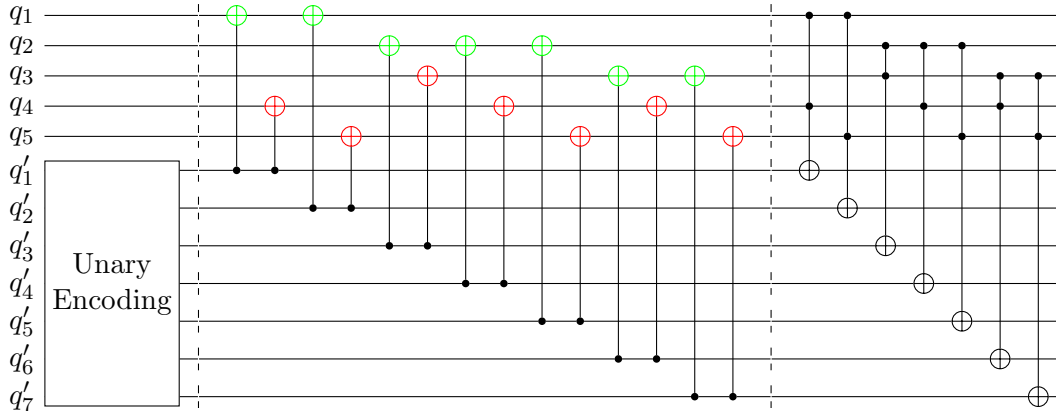


Figure 8: The circuit for preparing $|\psi_G\rangle$, where G is shown in Figure 7. In the middle stage, CNOT gates with the same color can be applied in depth $O(\log m)$.

5 Algorithms for preparing special graph structured states without ancillary qubits

In this section, we will introduce more algorithms for graphs with special structures. The advantage of these algorithms is that they do not use any ancillary qubits. Before that, another two methods to optimize the depth of CNOT circuits will be came up with beside the chain-like CNOT circuits introduced in Section 2.

5.1 Depth optimization for CNOT circuits

One approach is for a specific kind of CNOT circuit, called bipartite CNOT circuits. The qubits in a bipartite CNOT circuit can be divided into two parts $A = \{q_{a_1}, q_{a_2}, \dots, q_{a_n}\}$ and $B = \{q_{b_1}, q_{b_2}, \dots, q_{b_{n'}}\}$, and every CNOT gate must be controlled by a qubit in A and target on a qubit in B . Thus, this kind of CNOT circuits can be described by the corresponding directed bipartite graph $\{A \sqcup B, E\}$, where $q_{a_i}q_{b_j} \in E$ iff there is a CNOT gate controlled by q_{a_i} and targeting on q_{b_j} in the circuit. Again, we set $m = |E|$. We can also give a matrix representation of a bipartite CNOT circuit. Let $\vec{u}_A = (x_{a_1}, x_{a_2}, \dots, x_{a_n}) \in \mathbb{F}_2^n$ be some computational basis on qubits in A . Similarly, let $\vec{u}_B = (x_{b_1}, x_{b_2}, \dots, x_{b_{n'}}) \in \mathbb{F}_2^{n'}$ be some computational basis on qubits in B . Further let $M \in \mathbb{F}_2^{n' \times n}$, then $(\vec{u}_A, \vec{u}_B) \rightarrow (\vec{u}_A, \vec{u}_B + M\vec{u}_A)$ can be seen as a CNOT circuit based on a directed bipartite graph. Figure 9 is an example of a bipartite CNOT circuit with 6 CNOT gates.



Figure 9: A CNOT circuit and its corresponding bipartite graph.

It is obvious that all the CNOT gates in the circuit commute with each other, which means that the order of those CNOT gates does not matter. Suppose we also get l dirty ancillary qubits, here a dirty qubit means a qubit which state is unknown in the very beginning, and there are m CNOT gates in total.

Lemma 8 *When using l dirty ancillary qubits, any bipartite CNOT circuit with m edges can be implemented by a circuit with $O(\frac{m}{l} \log l)$ -depth and $O(m)$ -size.*

Proof. Because the order of these CNOT gates does not matter, we plan to apply l CNOT gates from the m CNOT gates in depth $O(\log l)$ (the l CNOT gates can be chosen in any way), so that the entire circuit can be implemented in a depth of $O(\frac{m}{l} \log l)$.

We name the l CNOT gates as $S = \{CX_1, CX_2, \dots, CX_l\}$ (note that S can also be treated as an operator by applying all the gates inside S), and name the l dirty ancillary qubits $\{q'_1, q'_2, \dots, q'_l\}$. For CX_j , which is controlled by some q_a and targets on some q_b , we turn it into 2 CNOT gates. One is controlled by q_a and targets on q'_j , named as CX_j^a , and the other one is controlled by q'_j and targets on q_b , named as CX_j^b . It is obvious that the original CX_j is not equivalent to CX_j^a followed by CX_j^b when q_j is dirty, so we have to do something more complicated.

We denote the set of all CX_j^a as S_A , the set of all CX_j^b as S_B . Again, all the CNOT gates in S_A commute with each other, so do the gates in S_B . Thus, we can apply all gates in $S_A(S_B)$ without concerning the order of applying those CNOT gates. We further notice that S_A consists of a group of independent fan-in gates, while S_B consists of a group of independent fan-out gates, and every single fan-in (out) gate concerns less than $n + 1$ qubits. This means that we can apply S_A and S_B both in a depth of $O(\log l)$. But how to apply S by using S_A and S_B ? The answer is $S = S_A S_B S_A S_B$. The proof for the correctness of the former formula is not difficult either.

Let us just consider the value on q_a, q'_j, q_b step by step when applying $S_A S_B S_A S_B$, and check if the final state coincides with CX_j

$$\begin{aligned}
& |x_a\rangle |x'_j\rangle |x_b\rangle \\
\xrightarrow{S_B} & |x_a\rangle |x'_j\rangle |x_b \oplus x'_j\rangle \\
\xrightarrow{S_A} & |x_a\rangle |x'_j \oplus x_a\rangle |x_b \oplus x'_j\rangle \\
\xrightarrow{S_B} & |x_a\rangle |x'_j \oplus x_a\rangle |x_b \oplus x_a\rangle \\
\xrightarrow{S_A} & |x_a\rangle |x'_j\rangle |x_b \oplus x_a\rangle.
\end{aligned} \tag{11}$$

The final state is exactly the output of CX_j ! Hence, we can apply S in $O(\log l) + O(\log l) + O(\log l) + O(\log l) = O(\log l)$ -depth and $O(l)$ -size. Thus the bipartite CNOT circuit can be implemented in $O(\frac{m}{l} \log l)$ -depth and $O(\frac{m}{l} l) = O(m)$ -size. \square

Obviously, the larger l in Lemma 8 is, the more significantly the circuit depth can be reduced. As a result, we will employ as many ancillary qubits as possible in later operations.

The second approach is for general CNOT circuits. Here we prove that any CNOT circuit on n qubits can be implemented in a depth of $O(\log n)$ with $O(n^2)$ dirty ancillary qubits.

Lemma 9 *When using $O(n^2)$ dirty ancillary qubits, any CNOT circuit on n qubits can be implemented by a circuit with $O(\log n)$ -depth.*

Proof. Assume the matrix representation of a general CNOT circuit is $M \in \mathbb{F}_2^{n \times n}$. Because M is invertible, M could be decomposed into $M = P^{-1}JP$, where P is invertible and J is the Jordan matrix whose diagonal elements are all 1.

Given an input $\vec{x} = (x_1, x_2, \dots, x_n) \in \mathbb{F}_2^n$, we wish the output could be $M\vec{x}$. We first take n dirty ancillary qubits, and suppose the value on these n ancillary qubits is $\vec{y} = (y_1, y_2, \dots, y_n) \in \mathbb{F}_2^n$.

We can solve this problem by the following steps.

$$\begin{aligned}
& (\vec{x}, \vec{y}) \\
\stackrel{1}{\longrightarrow} & (\vec{x}, \vec{y} + P\vec{x}) \\
\stackrel{2}{\longrightarrow} & (\vec{x} + P^{-1}(\vec{y} + P\vec{x}), \vec{y} + P\vec{x}) = (P^{-1}\vec{y}, \vec{y} + P\vec{x}) \\
\stackrel{3}{\longrightarrow} & (P^{-1}\vec{y}, \vec{y} + P\vec{x} + P(P^{-1}\vec{y})) = (P^{-1}\vec{y}, P\vec{x}) \\
\stackrel{4}{\longrightarrow} & (P^{-1}\vec{y}, JP\vec{x}) \\
\text{repeat 1,2,3} \longrightarrow & (P^{-1}JP\vec{x}, \vec{y}) = (M\vec{x}, \vec{y}).
\end{aligned} \tag{12}$$

Here, step 1, 2, 3 are bipartite CNOT circuits. In step 1 and 3, working qubits are control qubits and ancillary qubits are target qubits, and they shift the roles in step 2. As there are at most $n \times n = n^2$ edges in each bipartite graph, if we introduce $O(n^2)$ more ancillary qubits, step 1, 2, 3 can be implemented in a depth of $O(\frac{n^2}{n^2} \log n^2) = O(\log n)$. What we implement in step 4, are several independent CNOT circuits, and each circuit is an inversion of a chain-like CNOT circuit, so the depth of step 4 is also $O(\log n)$. Therefore the overall depth is $O(\log n)$. \square

5.2 The preparation algorithm for the tree-structured states without ancillary qubits

Before we present the preparation algorithm, it is necessary to review a significant property of trees.

Lemma 10 ([Die17]) *For every tree G with n vertices where $n \geq 3$, there exists a vertex v , such that every connected component in $G - v$ has less than $(n - 1)/2$ edges and no more than $n/2$ vertices.*

We can get a corollary from this lemma.

Corollary 1 *For every tree $G = (V, E)$ with n vertices and $r < n$, there exists a vertex set $V' \subset V$, such that $|V'| \leq 2r$ and every connected component in $G - V'$ has no more than n/r vertices.*

Proof. Here we only prove when $r = 2^t$ is a power of 2. We prove it by induction on t .

When $t = 1$, the claim is correct using the lemma above directly. Assume the claim is correct when $r = 2^s$. For $t = s+1$, by induction, we already have a vertex set $V'' \subset V$, such that $|V''| \leq 2 \cdot 2^s$ and every connected component in $G - V''$ has no more than $n/2^s$ vertices. But there may exist connected component in $G - V''$ that has more than $n/2^{s+1}$ vertices. The number of this kind of connected component will be no more than 2^{s+1} . By Lemma 10, we can add the center of this kind of connected component in to V'' and hence get a new vertex set V' , obviously every connected component in $G - V'$ has no more than $n/2^{s+1}$ vertices now. Besides, $|V'| \leq |V''| + 2^{s+1} \leq 2 \cdot 2^{s+1}$, so we are done. \square

Now we are ready to show the circuit that prepares a tree-structured state in depth $O(\log n)$ without ancillary qubits.

Algorithm 2 Preparation of tree-structured states without ancillary qubits.

Input: An arbitrary tree $G = (V, E)$, where $n = |V|$; n working qubits.

Output: The circuit that prepares $|\psi_G\rangle$.

- 1: Choose v_1 as the root of G , then every edge in G has a father node and a child node, and every node has a height h . Denote the height of G as H .
- 2: Apply Unary Encoding on $\{q_2, q_3, \dots, q_n\}$, and note the qubit q_j corresponds to the node v_j . The coefficient of $|e_j\rangle$ is (the weight of the edge of which v_j is playing as the child node)/ \sqrt{M} .
- 3: **for** $h = 1$ to H **do**
- 4: For every node v_j which height is h , apply a CNOT gate controlled by v_j and targeting on its father node.
- 5: **end for**
- 6: Return the whole circuit.

Lemma 11 *Algorithm 2 can correctly prepare a tree-structured state.*

Proof. After line 1 and 2, the state becomes

$$\frac{1}{\sqrt{M}} \sum_{v_i v_j \in E, v_j \text{ is the child node of this edge}} w_{ij} |e_j\rangle. \quad (13)$$

Except for the root node (v_1), every node will be playing as the child node exactly once, so the state above is well defined.

For every CNOT gate applied between line 3 to 5, take the CNOT gate controlled by v_j and targeting on its father node, v_i as an example, the only change that this CNOT gate makes is that it turns $|e_j\rangle$ into $|e_i \oplus e_j\rangle$. Thus, the whole circuit between line 3 to 5 successfully turns all $|e_j\rangle$ into $|e_i \oplus e_j\rangle$. Hence the state becomes

$$\frac{1}{\sqrt{M}} \sum_{v_i v_j \in E, v_j \text{ is the child node of this edge}} w_{ij} |e_i \oplus e_j\rangle, \quad (14)$$

which is exactly what we want. \square

An example is shown in Figure 10. In this example, we aim to prepare the state $|\psi_G\rangle = \frac{1}{\sqrt{13}}(\sqrt{1}|1100000\rangle + \sqrt{2}|1010000\rangle + \sqrt{2}|0101000\rangle + \sqrt{3}|0100100\rangle + \sqrt{3}|0010010\rangle + \sqrt{2}|0010001\rangle)$. The first term in the right hand of Figure 10 means the Unary Encoding circuit. The coefficient of a non-root node is set to the weight of the edge in which the node is playing as the son node. The second term means the CNOT gates circuits followed by the Unary Encoding circuit, the arrow means the CNOT gate controlled by the start of the arrow and targeting on the end of the arrow. The order of these CNOT gates matters. CNOT gates shown in solid arrows should be applied first, and the dashed arrows follow.

Theorem 8 *(Restatement of Theorem 2) For an arbitrary tree G with n vertices, $|\psi_G\rangle$ can be prepared by a circuit with $O(\log n)$ -depth without ancillary qubits.*

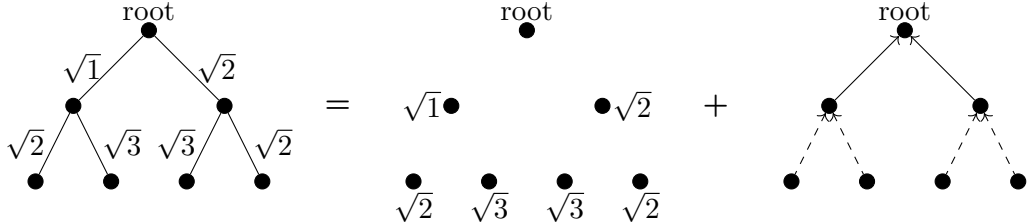


Figure 10: Algorithm for preparing tree-structured states, and nodes are labelled in level order (although the order does not really matter, we set this order just to match the state described in the text).

Proof. Line 1 and 2 is the Unary Encoding circuit, which can be implemented in a depth of $O(\log n)$.

For the circuit between line 3 to 5, we are actually applying a tree-shape CNOT circuit. For every edge in G , we apply a CNOT gate controlled by child node and targeting on father node. But here the order matters. We have to apply these CNOT gates from top to bottom.

Here we consider the inverse of this circuit, and call it U . This means we are facing a circuit that apply these CNOT gates from bottom to top. Note that after applying U , the value on a single node is the sum of all the original value of its descendent and its original value.

We hope to solve this problem by recursion. By using Corollary 1, we can find a vertex set $V' \subset V$, such that $|V'| \leq 2r$ and every connected component in $G - V'$ has no more than n/r vertices. If we correctly set all the values of vertices in $|V'|$ and further apply all the CNOT gates controlled by vertex in $|V'|$, then we successfully delete these vertices from the whole circuit, and for the rest of the CNOT circuit, we can implement all the connected components independently. The process of deleting these vertices can be divided into 3 steps.

Step 1: For $\forall v_j \in V'$ define $V_j = \{v_i : v_i$ is a descendant of v_j and the inner vertices in the path from v_j to v_i do not have vertices in $V'\}$, and then apply a fan-in gate from V_j to v_j . It's obvious that all the V_j are independent from each other. So the whole depth of step 1 is $O(\log n)$.

Step 2: Make a new CNOT circuit inside V' : there is a CNOT gate controlled by $v_i \in V'$ and targeting on $v_j \in V'$ iff v_i is a descendant of v_j and the inner vertices in the path from v_j to v_i do not have vertices in V' . The sequence is also from bottom to top. We can find that after this step, all of $v_j \in V'$ has possessed the correct value. Further more, the new CNOT circuit created in this step is applied on $2r$ vertices. The good news is that, based on Corollary 1, when we set $r = \sqrt{n}$, all the other qubits could be used as dirty ancillary qubit. We can take out $O((\sqrt{n})^2) = O(n)$ vertices as dirty ancillary qubits, so that the new CNOT circuit can be implemented in a depth of $O(\log n)$.

Step 3: For $\forall v_j \in V'$, apply a CNOT gate controlled by v_j and targeting on the father node of v_j if the father node is not in V' . This is a group of independent fan-in gates, so step 3 can be implemented in a depth of $O(\log n)$.

As a result, the entire process can be implemented in a depth of $O(\log n)$.

If we denote the depth of the tree-shape CNOT circuit as $f(n)$, by setting $r = \sqrt{n}$, we can get

$f(n) = O(\log n) + f(\sqrt{n})$. Hence $f(n) = O(\log n)$. Together with the former Unary Encoding, we can claim that tree-structured states can be prepared in a depth of $O(\log n) + O(\log n) = O(\log n)$. \square

5.3 The preparation algorithm for the grid-structured states without ancillary qubits

Compared to the vertex in the tree graph with explicit layer structure (parent and child, ancestor and descendant), the nodes in the grid graph have no similar relations, which leads to the difficulty to implement appropriate Unary Encoding directly. Therefore, we consider doing some pretreatment and applying the inverse circuit. This kind of method has appeared in other QSP problems [GH21].

Before introducing the algorithm, we first consider the effect of a controlled- $RBS(\theta)$ gate. Assume that q_1 is controlling an $RBS(\theta)$ gate on q_2, q_3 . When we just consider the computational basis with Hamming weight 2, besides a trivial input $|0\rangle^{\otimes n}$, we can find that the controlled- $RBS(\theta)$ gate will only affect $|e_1 \oplus e_2\rangle$ and $|e_1 \oplus e_3\rangle$, while keeping all other possible inputs unchanged. $|e_1 \oplus e_2\rangle$ will turn into $\cos \theta |e_1 \oplus e_2\rangle + \sin \theta |e_1 \oplus e_3\rangle$. $|e_1 \oplus e_3\rangle$ will turn into $|e_1 \oplus e_2 \oplus e_3\rangle$, which is a bad result (we do not want a base with Hamming weight more than 2). As a result, when the input of the circuit is a state with graph structure G , and $v_1v_2 \in G, v_1v_3 \notin G$, the output will be the state with graph structure $G' = G + v_1v_3$, the weight of v_1v_2 in G will be split by the new edge v_1v_3 in G' , and the proportion is determined by θ in the controlled- $RBS(\theta)$ gate. So the controlled- $RBS(\theta)$ gate can be treated as “edge generator”, as long as the edge we want to add into the graph already has an adjacent edge in the original graph. On the other hand, the inverse of the controlled- $RBS(\theta)$ gate is “deleting” an edge (and bringing its weight to one of its adjacent edge) in G . Note that a controlled- $RBS(\theta)$ gate (and its inverse) has a constant size and depth.

In this subsection, we prepare the $s \times t$ -grid-structured state, and denote the vertex in the i^{th} row and the j^{th} column as $v_{i,j}$, and $q_{i,j}$ means the corresponding qubit. The pseudocode is shown in Algorithm 3.

Algorithm 3 The inverse circuit of preparing grid-structured states without ancillary qubits.

Input: An arbitrary $s \times t$ grid $G = (V, E)$, where $n = st = |V|$; n working qubits.

Output: The circuit that turns $|\psi_G\rangle$ into $|0\rangle^{\otimes n}$.

```

1: procedure GRIDCUT( $s, t, s \times t$  grid  $G$ )
2:   if  $t \geq 3$  then
3:     for  $k = 1$  to  $s$  do
4:       Apply a inverse gate of the controlled- $RBS(\theta)$  gate on  $q_{k,\lfloor t/2 \rfloor}, q_{k,\lfloor t/2 \rfloor+1}, q_{k,\lfloor t/2 \rfloor+2}$ ,
       so that the edge  $v_{k,\lfloor t/2 \rfloor}v_{k,\lfloor t/2 \rfloor+1}$  is deleted.
5:     end for
6:   We have cut  $G$  into 2 small grids, we name the left one  $G_1$  and right one  $G_2$ .
7:   GRIDCUT( $s, \lfloor t/2 \rfloor, G_1$ )
8:   GRIDCUT( $s, t - \lfloor t/2 \rfloor, G_2$ )

```

```

9:   else if  $s \geq 3$  then
10:    We do exactly the same work as line 3 to 4 by cutting  $G$  into a top grid  $G_1$  and a bottom
    grid  $G_2$ .
11:    GRIDCUT( $\lfloor s/2 \rfloor$ ,  $t$ ,  $G_1$ )
12:    GRIDCUT( $s - \lfloor s/2 \rfloor$ ,  $t$ ,  $G_2$ )
13:   else if  $t = s = 2$  then
14:    Delete  $v_{(1,1)}v_{(2,1)}, v_{(2,1)}v_{(2,2)}, v_{(2,2)}v_{(1,2)}$  by applying 3 inverse gates of the controlled-
     $RBS(\theta)$  gates.
15:   end if
16:   Return;
17: end procedure
18:
19: GRIDCUT( $s$ ,  $t$ ,  $G$ ), after which the final graph consists of independent edges.
20: For every edge in the graph, apply a CNOT gate controlled by one end and targeting on the
    other end.
21: Apply the inverse circuit of the Unary Encoding circuit.
22: Return the whole circuit.

```

Lemma 12 *Algorithm 3 correctly turns $|\psi_G\rangle$ into $|0\rangle^{\otimes n}$.*

Proof. Let's just consider what we have done in a single GridCut ($s, t, s \times t$ grid G) function. If $t \geq 3$ or $s \geq 3$, we simply remove all the edges in the middle. If G is a 2×2 grid, we delete 3 edges so that there is only 1 edge left. As a result, after line 19, the final graph consists of independent edges. Assume the state after line 19 is of the form $\sum_{v_i v_j \in G_{\text{final}}} w'_{ij} |e_i \oplus e_j\rangle$. After line 20 the state becomes $\sum_{v_i v_j \in G_{\text{final}}} w'_{ij} |e_j\rangle$, this is exactly the form of states after Unary Encoding. Hence we just apply the inverse of Unary Encoding (line 21) to get $|0\rangle^{\otimes n}$. \square

Theorem 9 *(Restatement of Theorem 3) For an arbitrary grid G with n vertices, $|\psi_G\rangle$ can be prepared by a circuit with $O(\log n)$ -depth without ancillary qubits.*

Proof. In a single GridCut($s, t, s \times t$ grid G) function, if $t \geq 3$, we simply remove all the edges in the middle. As different controlled- $RBS(\theta)$ gates work on different qubits, line 3 and 4 only needs a depth $O(1)$. After we remove those edges, we get 2 small grids, G_1, G_2 . It is obvious that the number of vertices in each small grid is approximately $n/2$, here we can use a very loose upper bound. The number of vertices in each small grid is smaller than $\frac{2}{3}n$. As G_1 and G_2 are independent from each other, line 11 and line 12 can work in parallel. The same analysis holds when $s \geq 3$. If we denote the depth of a GridCut function of a n -vertex grid as $f(n)$, we get $f(n) \leq O(1) + f(\frac{2}{3}n)$. So $f(n) = O(\log n)$. As a result, line 20 needs a depth of $O(\log n)$, line 21 needs a depth of 1, and line 19 needs a depth of $O(\log n)$, so that the whole depth is $O(\log n)$. \square

Figure 11 is an example to show how Algorithm 3 works on a 3×4 grid. Starting from $|\psi_G\rangle$, we first apply GridCut($3, 4, G$), so that we actually apply 3 inverse gates of controlled- $RBS(\theta)$

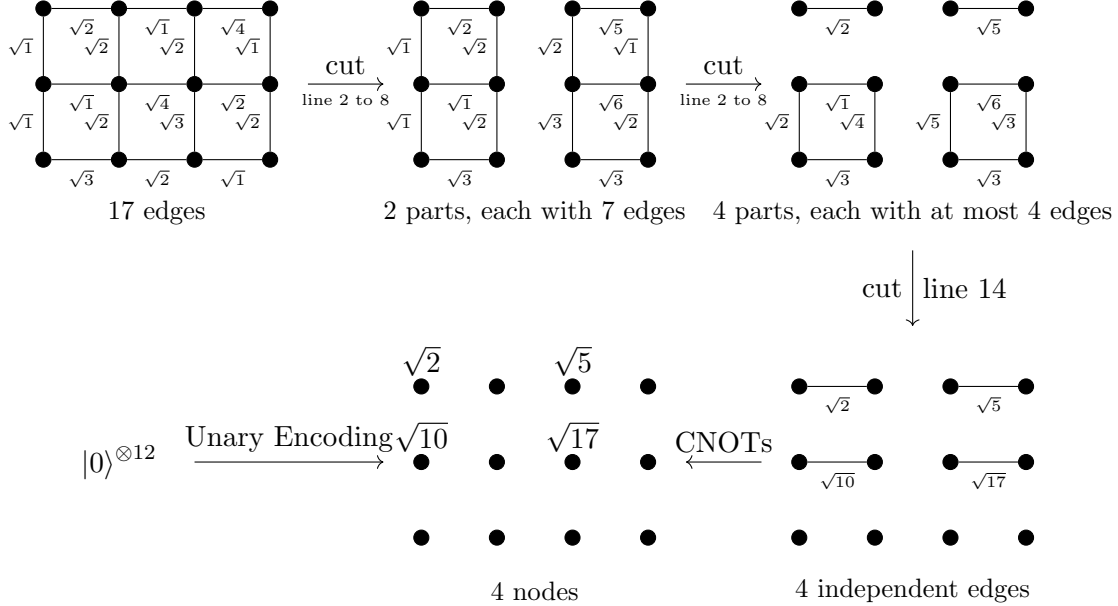


Figure 11: An example of preparing a 3×4 grid-structured state.

gates, and cut the entire grid into two small grids G_1 and G_2 . Then we can apply $\text{GridCut}(3, 2, G_1)$ and $\text{GridCut}(3, 2, G_2)$ simultaneously. After 3 rounds of GridCut, we only have independent edges and nodes. For every edge, we apply a CNOT gate controlled by one end and targeting on the other end, so that the state we get is exactly the result of a Unary Encoding circuit.

6 Algorithm for preparing Hamming-Weight-preserving states with ancillary qubits

In this section, we introduce the algorithm for preparing a Hamming-Weight-preserving state with $O(\log \binom{n}{k})$ -depth using $O(\binom{n}{k})$ ancillary qubits. Before that, we will first show a weaker algorithm, which is a direct generalization of Algorithm 1.

Lemma 13 *For any HWP quantum state with parameters n and k , it can be prepared by a circuit with $O(\log \binom{n}{k})$ -depth and $O(k \binom{n}{k})$ -size using $O(k \binom{n}{k})$ ancillary qubits.*

Proof. This algorithm is quite similar to Algorithm 1. We first apply the Unary Encoding on $\binom{n}{k}$ ancillary qubits. Each ancillary qubit q'_x represents a computational basis in $|\psi_{HWP}\rangle$. This step needs $\binom{n}{k}$ ancillary qubits, and has $O(\log \binom{n}{k})$ -depth and $O(\binom{n}{k})$ -size. We get the following transformation.

$$|0\rangle^{\otimes n} |0\rangle^{\otimes \binom{n}{k}} \xrightarrow{\text{Unary Encoding}} |0\rangle^{\otimes n} \sum_{\text{HW}(x)=k} \alpha_x |e_x\rangle. \quad (15)$$

Next, for each q'_x , we apply CNOT gates controlled by q'_x and targeting on all the q_i s that the i^{th} digit of x is 1. Because $\text{HW}(x) = k$, k CNOT gates are applied here. As a result, there are $k \binom{n}{k}$ CNOT gates in total. This CNOT circuit is obviously a bipartite CNOT circuit. By Lemma 8, when using $k \binom{n}{k}$ ancillary qubits, this CNOT circuit can be implemented with $O(\log k \binom{n}{k}) = O(\log \binom{n}{k})$ -depth and $O(k \binom{n}{k})$ -size. We get the following transformation.

$$|0\rangle^{\otimes n} \sum_{\text{HW}(x)=k} \alpha_x |e_x\rangle \xrightarrow{\text{CNOTs}} \sum_{\text{HW}(x)=k} \alpha_x |x\rangle |e_x\rangle. \quad (16)$$

Finally, for each q'_x , we apply a $C^k X$ gate targeting on q'_x and controlled by all the q_i s that the i^{th} digit of x is 1. There are $\binom{n}{k} C^k X$ gates in total. For each q_i , it is associated with $\binom{n-1}{k-1} C^k X$ gates. We make $\binom{n-1}{k-1}$ copies of each q_i , so that all $\binom{n}{k} C^k X$ gates can be applied simultaneously. Then we apply the inverse of the copying stage. In the copying (together with the inverse) stage, we make $n \binom{n-1}{k-1} = k \binom{n}{k}$ copies in total, so we add $k \binom{n}{k}$ ancillary qubits and take $O(\log k \binom{n}{k}) = O(\log \binom{n}{k})$ -depth and $O(k \binom{n}{k})$ -size. Next in the $C^k X$ stage, by Lemma 1, we add $\binom{n}{k}$ ancillary qubits and take $O(k)$ -depth and $O(k \binom{n}{k})$ -size. We get the following transformation.

$$\sum_{\text{HW}(x)=k} \alpha_x |x\rangle |e_x\rangle \xrightarrow{C^k(X)s} \left(\sum_{\text{HW}(x)=k} \alpha_x |x\rangle \right) |0\rangle^{\otimes \binom{n}{k}}. \quad (17)$$

In aggregate, this circuit uses $O(k \binom{n}{k})$ ancillary qubits, and has $O(\log \binom{n}{k})$ -depth and $O(k \binom{n}{k})$ -size. \square

Obviously, the above algorithm is very similar to the Algorithm 1, and the only difference is the number of controlled qubits. Precisely because here the number of controlled qubits in the CNOT stage and the $C^k X$ stage is k rather than 2, the final size complexity exceeds the expected $O(\binom{n}{k})$.

However, the circuit shown in Lemma 13 will become an important sub-circuit in the following Algorithm 4, which can prepare the HWP states in $O(\binom{n}{k})$ -size and $O(\log \binom{n}{k})$ -depth simultaneously. Before that, we need to introduce a representation of the decimal number x in Lemma 14, and explain the necessary registers of ancillary qubits, which play key roles in the preparation algorithm design.

Lemma 14 *For all $x, i \in \mathbb{N}$ with $0 \leq x \leq 2^n - 1$ and $1 \leq i \leq n$, there exists a unique ordered pair (a, b) satisfying $a, b \in \mathbb{N}$ with $0 \leq a \leq 2^i - 1$ and $0 \leq b \leq 2^{n-i} - 1$ so that $x = 2^{n-i}a + b$. In quantum computation, this can be written as $|x\rangle = |a\rangle |b\rangle$.*

Proof. This follows straightforwardly from the division algorithm. \square

Next we recommend the ancillary qubits, which have been separated into different registers. For simplicity, we assume that k is an even number. Register A contains $\binom{n}{k}$ ancillary qubits, and each qubit q'_x represents a computational basis in $|\psi_H\rangle$. Register B contains several small registers $B_{\frac{k}{2}}, B_{\frac{k}{2}+1}, \dots, B_{n-\frac{k}{2}}$, where B_i contains $\binom{i}{\frac{k}{2}} + \binom{n-i}{\frac{k}{2}}$ ancillary qubits. In B_i , each qubit in the first $\binom{i}{\frac{k}{2}}$ qubits represents an i -bit string with Hamming Weight $\frac{k}{2}$, and each qubit in the last $\binom{n-i}{\frac{k}{2}}$

qubits represents a $(n - i)$ -bit string with Hamming Weight $\frac{k}{2}$. Register C contains several small registers $C_{\frac{k}{2}}, C_{\frac{k}{2}+1}, \dots, C_{n-\frac{k}{2}}$, where C_i contains n ancillary qubits. Register D, E, F each contains $n - k + 1$ qubits respectively. Each qubit in register D represents a position in an n -bit string, starting with the $\frac{k}{2}^{th}$ place and ending with the $(n - \frac{k}{2})^{th}$ place. Now we are ready to present the preparation algorithm for HWP states, as shown in Algorithm 4.

Algorithm 4 Preparation of a Hamming-Weight-preserving state with $O\left(\binom{n}{k}\right)$ ancillary qubits.

Input: $n; k; \binom{n}{k}$ coefficients $\{\alpha_x\}$.

Output: The circuit that prepares $|\psi_H\rangle$.

- 1: Apply Unary Encoding on register A , where the coefficients are from $\{\alpha_x\}$.
- 2: **for** every x with $\text{HW}(x) = k$ **do**
- 3: Calculate the position of the $\frac{k}{2}^{th}$ 1 in x (from left to right), denote as i . By Lemma 14, find (a, b) so that $|x\rangle = |a\rangle |b\rangle$. By the choice of i , both a and b have a Hamming Weight of $\frac{k}{2}$.
- 4: Apply 2 CNOT gates both controlled by q'_x in register A , and targeting on the qubits representing a and b in register B_i .
- 5: Apply 1 CNOT gate controlled by q'_x , and targeting on the qubit representing i in register D .
- 6: **end for**
- 7: **for** every edge x with $\text{HW}(x) = k$ **do**
- 8: Apply a Toffoli gate controlled by the qubits representing a and b in register B_i , targeting on q'_x .
- 9: **end for**
- 10: **for** every register B_i in register B **do**
- 11: Apply the circuit (except for the Unary Encoding step) introduced in Lemma 13 to the first $\binom{i}{\frac{k}{2}}$ qubits and the last $\binom{n-i}{\frac{k}{2}}$ qubits respectively, and store the result in register C_i .
- 12: **end for**
- 13: **for** every register C_i in register C **do**
- 14: Apply n CNOT gates: for all $j \in [n]$, the j^{th} CNOT gate is controlled by the j^{th} qubit in C_i and targeting on the working qubit q_j .
- 15: **end for**
- 16: **for** every register C_i in register C **do**
- 17: Apply n Toffoli gates: for all $j \in [n]$, the j^{th} Toffoli gate is controlled by the working qubit q_j and the qubit representing i in register D , and targeting on the j^{th} qubit in C_i .
- 18: **end for**
- 19: Make $n - k + 1$ copies of the working qubits and index them as: $\frac{k}{2}, \frac{k}{2} + 1, \dots, n - \frac{k}{2}$.
- 20: **for** j from $\frac{k}{2}$ to $n - \frac{k}{2}$ **do**
- 21: Apply an HWC gate on the first j qubit of the j^{th} copy of the working qubits to check if the Hamming Weight equals $\frac{k}{2}$, and store the result in register E .
- 22: **end for**
- 23: Apply an HWC gate on register E to check if the Hamming Weight equals 1, and store the

result in a single ancillary qubit q^* .

24: **if** $q^* = 1$ **then**

25: Apply $n - k + 1$ CNOT gates: for all j from $\frac{k}{2}$ to $n - \frac{k}{2}$, the j^{th} CNOT gate is controlled by the j^{th} qubit in E and targeting on the j^{th} qubit in D .

26: All the operations in this situation should be controlled by q^* when $q^* = 1$.

27: **else**

28: Make $n - k + 1$ copies of register E and index them as: $\frac{k}{2}, \frac{k}{2} + 1, \dots, n - \frac{k}{2}$.

29: **for** j from $\frac{k}{2}$ to $n - \frac{k}{2}$ **do**

30: Apply HWC on the first j qubit of the j^{th} copy of register E to check if the Hamming Weight equals 1, and store the result in register F .

31: **end for**

32: Apply $n - k + 1$ CNOT gates: for all j from $\frac{k}{2}$ to $n - \frac{k}{2}$, the j^{th} CNOT gate is controlled by the j^{th} qubit in F and targeting on the j^{th} qubit in D .

33: Apply the inverse circuit from line 28 to line 31.

34: All the operations in this situation should be controlled by q^* when $q^* = 0$.

35: **end if**

36: Apply the inverse circuit from line 19 to line 23.

37: Return the whole circuit.

Lemma 15 *Algorithm 4 can correctly prepare the Hamming-Weight-preserving state.*

Proof. Line 1 is the Unary Encoding circuit. From line 2, we analyze the circuit by considering each possible input rather than the whole state for simplicity. Actually, the transformation of the whole state is the linear combination of that of each possible input, which does not affect neither the correctness nor the complexity of the algorithm. The following is the transformation process of one possible input, which can be derived through straightforward computation. It is noteworthy that we may omit some unchanged ancillary registers and abbreviate the initial state to $|0\rangle$ on them in the process.

$$\begin{aligned}
& \underbrace{|0\rangle^{\otimes n}}_{\text{working}} \underbrace{|e_x\rangle}_A \\
\xrightarrow{\text{line 2 to 6}} & \underbrace{|0\rangle^{\otimes n}}_{\text{working}} \underbrace{|e_x\rangle}_A \underbrace{(|0\rangle \dots |e_a\rangle |e_b\rangle \dots |0\rangle)}_{B_i} \underbrace{|e_i\rangle}_{D} \\
\xrightarrow{\text{line 7 to 9}} & \underbrace{|0\rangle^{\otimes n}}_{\text{working}} \underbrace{|0\rangle}_A \underbrace{(|0\rangle \dots |e_a\rangle |e_b\rangle \dots |0\rangle)}_{B_i} \underbrace{|e_i\rangle}_{D} \\
\xrightarrow{\text{line 10 to 12, discard } A} & \underbrace{|0\rangle^{\otimes n}}_{\text{working}} \underbrace{(|0\rangle \dots |0\rangle |0\rangle)}_{B_i} \underbrace{(|0\rangle \dots |x\rangle \dots |0\rangle)}_{C_i} \underbrace{|e_i\rangle}_{D} \\
\xrightarrow{\text{line 13 to 15, discard } B} & \underbrace{|x\rangle}_{\text{working}} \underbrace{(|0\rangle \dots |x\rangle \dots |0\rangle)}_{C_i} \underbrace{|e_i\rangle}_{D} \\
\xrightarrow{\text{line 16 to 18}} & \underbrace{|x\rangle}_{\text{working}} \underbrace{(|0\rangle \dots |0\rangle \dots |0\rangle)}_{C_i} \underbrace{|e_i\rangle}_{D} \\
\xrightarrow{\text{discard } C} & \underbrace{|x\rangle}_{\text{working}} \underbrace{|e_i\rangle}_D \\
\xrightarrow{\text{line 19}} & \underbrace{|x\rangle \dots |x\rangle}_{(n-k+1)\text{times}} \underbrace{|e_i\rangle}_D.
\end{aligned} \tag{18}$$

The next task is to restore the state in register D to $|0\rangle$. Based on the $(n - k + 1)$ copies of $|x\rangle$, Line 20 to 22 checks the Hamming Weight of prefixes of $|x\rangle$, and register E will be the form $|0 \dots 01 \dots 10 \dots 0\rangle$. The place of the first “1” in register E means the prefix ending with this place first has Hamming Weight $\frac{k}{2}$, so this place is exactly i mentioned in line 3. If there is only one “1” in register E , the value on q^* will be 1, and register E equals register D . The process continues by the following transformation:

$$\begin{aligned}
& \underbrace{|x\rangle \dots |x\rangle}_{(n-k+1)\text{times}} \underbrace{|e_i\rangle}_D \\
\xrightarrow{\text{line 20 to 22}} & \underbrace{|x\rangle \dots |x\rangle}_{(n-k+1)\text{times}} \underbrace{|e_i\rangle}_D \underbrace{|e_i\rangle}_E \underbrace{|0\rangle}_{q^*} \\
\xrightarrow{\text{line 23}} & \underbrace{|x\rangle \dots |x\rangle}_{(n-k+1)\text{times}} \underbrace{|e_i\rangle}_D \underbrace{|e_i\rangle}_E \underbrace{|1\rangle}_{q^*} \\
\xrightarrow{\text{line 25 to 26}} & \underbrace{|x\rangle \dots |x\rangle}_{(n-k+1)\text{times}} \underbrace{|0\rangle}_D \underbrace{|e_i\rangle}_E \underbrace{|1\rangle}_{q^*} \\
\xrightarrow{\text{line 36}} & \underbrace{|x\rangle}_{\text{working}} \underbrace{|0\rangle}_D \underbrace{|0\rangle}_E \underbrace{|0\rangle}_{q^*} .
\end{aligned} \tag{19}$$

If there is more than one “1” in register E , the value on q^* will be 0. By checking the prefixes of register E , line 28 to 31 successfully removes the “1”s after the first “1” in register E and put the new binary string into register F . The process continues by the following transformation:

$$\begin{aligned}
& \underbrace{|x\rangle \dots |x\rangle}_{(n-k+1)\text{times}} \underbrace{|e_i\rangle}_D \\
\xrightarrow{\text{line 20 to 22}} & \underbrace{|x\rangle \dots |x\rangle}_{(n-k+1)\text{times}} \underbrace{|e_i\rangle}_D \underbrace{|0\dots 01\dots 10\dots 0\rangle}_{E \text{ (more than one “1”s)}} \underbrace{|0\rangle}_{q^*} \\
\xrightarrow{\text{line 23}} & \underbrace{|x\rangle \dots |x\rangle}_{(n-k+1)\text{times}} \underbrace{|e_i\rangle}_D \underbrace{|0\dots 01\dots 10\dots 0\rangle}_{E} \underbrace{|0\rangle}_{q^*} \\
\xrightarrow{\text{line 28}} & \underbrace{|x\rangle \dots |x\rangle}_{(n-k+1)\text{times}} \underbrace{|e_i\rangle}_D \underbrace{|0\dots 01\dots 10\dots 0\rangle^{\otimes n-k+1}}_{(n-k+1) \text{ copies of } E} \underbrace{|0\rangle}_{q^*} \\
\xrightarrow{\text{line 29 to 31}} & \underbrace{|x\rangle \dots |x\rangle}_{(n-k+1)\text{times}} \underbrace{|e_i\rangle}_D \underbrace{|0\dots 01\dots 10\dots 0\rangle^{\otimes n-k+1}}_{(n-k+1) \text{ copies of } E} \underbrace{|e_i\rangle}_F \underbrace{|0\rangle}_{q^*} \\
\xrightarrow{\text{line 32}} & \underbrace{|x\rangle \dots |x\rangle}_{(n-k+1)\text{times}} \underbrace{|0\rangle}_D \underbrace{|0\dots 01\dots 10\dots 0\rangle^{\otimes n-k+1}}_{(n-k+1) \text{ copies of } E} \underbrace{|e_i\rangle}_F \underbrace{|0\rangle}_{q^*} \\
\xrightarrow{\text{line 33}} & \underbrace{|x\rangle \dots |x\rangle}_{(n-k+1)\text{times}} \underbrace{|0\rangle}_D \underbrace{|0\dots 01\dots 10\dots 0\rangle}_{E} \underbrace{|0\rangle}_{q^*} \\
\xrightarrow{\text{line 36}} & \underbrace{|x\rangle}_{\text{working}} \underbrace{|0\rangle}_D \underbrace{|0\rangle}_E \underbrace{|0\rangle}_{q^*} .
\end{aligned} \tag{20}$$

As a result, in both cases, the final output of the circuit will be $|x\rangle$, while all ancillary qubits

are restored to $|0\rangle$. Thus, we finish the preparation of HWP states successfully. \square

Theorem 10 (Restatement of Theorem 4) *Based on Algorithm 4, for any HWP quantum state with parameters n and k , it can be prepared by a circuit with $O(\log \binom{n}{k})$ -depth using $O(\binom{n}{k})$ ancillary qubits.*

Proof. Line 1 is the Unary Encoding circuit, which has $O(\log \binom{n}{k})$ -depth and $O(\binom{n}{k})$ -size. From line 2 to 6, for every x with $\text{HW}(x) = k$, 3 CNOT gates controlled by q'_x are applied. There are $3\binom{n}{k}$ CNOT gates in this stage, and they form a bipartite CNOT circuit, by Lemma 8, when using $O(\binom{n}{k})$ ancillary qubits, this CNOT circuit can be implemented with $O(\log \binom{n}{k})$ -depth and $O(\binom{n}{k})$ -size.

From line 7 to 9, for every x with $\text{HW}(x) = k$, a Toffoli gate targeting on q'_x is applied. There are $\binom{n}{k}$ Toffoli gates in this stage. By copying $2\binom{n}{k}$ qubits in register B , these Toffoli gates can be applied simultaneously. We further apply the inverse of the copying stage. Overall, when using $2\binom{n}{k}$ more ancillary qubits, this Toffoli circuit can be implemented with $O(\log \binom{n}{k})$ -depth and $O(\binom{n}{k})$ -size.

From line 10 to 12, for every register B_i in register B , by Lemma 13, the circuit depth for every B_i is $O\left(\max\left(\log \binom{i}{2}, \log \binom{n-i}{2}\right)\right)$, which belongs to $O(\log \binom{n}{k})$. Because the circuits for B_i s can be applied simultaneously, the overall depth of this stage is $O(\log \binom{n}{k})$. Also by Lemma 13, the circuit size complexity for every B_i is $O\left(\frac{k}{2}\left(\binom{i}{2} + \binom{n-i}{2}\right)\right)$, hence the overall size complexity of this stage is $\sum_{i=\frac{k}{2}}^{n-\frac{k}{2}} O\left(\frac{k}{2}\left(\binom{i}{2} + \binom{n-i}{2}\right)\right)$. By some combinatorial identities and the following estimation,

$$\begin{aligned}
& \sum_{i=\frac{k}{2}}^{n-\frac{k}{2}} \left(\frac{k}{2} \left(\binom{i}{2} + \binom{n-i}{2} \right) \right) \\
&= k \binom{n - \frac{k}{2} + 1}{\frac{k}{2} + 1} \\
&\leq 4 \left(\lceil \frac{k}{4} \rceil \binom{n - \frac{k}{2} + 1}{\frac{k}{2} + 1} \right) \\
&\leq 4 \left(\sum_{i=0}^{\lceil \frac{k}{4} \rceil - 1} \binom{n - \frac{k}{2} + 1 + i}{\frac{k}{2} + 1} \right) \\
&\leq 4 \binom{n - \frac{k}{2} + \lceil \frac{k}{4} \rceil + 1}{\frac{k}{2} + 2} \\
&\leq 4 \binom{n}{k},
\end{aligned} \tag{21}$$

the overall size complexity of this stage is $O(\binom{n}{k})$.

From line 13 to 15, there are $n(n - k)$ CNOT gates in total, and this is again a bipartite CNOT circuit; from line 16 to 18, there are $n(n - k)$ Toffoli gates in total. By the same method concerning line 2 to 6 and line 7 to 9, line 13 to 18 can be implemented with $O(\log \binom{n}{k})$ -depth and $O(\binom{n}{k})$ -size.

Line 19 is a copying stage. We add $n(n - k)$ ancillary qubits, hence line 19 can be implemented with $O(\log n(n - k))$ -depth and $O(n(n - k))$ -size.

From line 20 to 22, we apply $n - k + 1$ HWC gates simultaneously. By Lemma 5, when using $O(n^2(n - k + 1))$ ancillary qubits, this stage can be implemented with $O(\log n)$ -depth and $O(n^2(n - k + 1))$ -size.

Line 23 is trivial. Line 25, together with line 28 to 32 is also trivial by using the methods mentioned above. However, it should be noted that the operations in line 25 and line 28 to 32 are controlled by q^* . By Lemma 2, they can still be implemented with $O(\log n)$ -depth and $O(n^2(n - k + 1))$ -size.

Line 36 is the inverse of some of the former operations and is therefore trivial.

We have analyzed the depth and size complexity of every stage in Algorithm 4, and all of them are upper bounded by $O(\log \binom{n}{k})$ -depth and $O(\binom{n}{k})$ -size. The only thing that has not been mentioned is the number of ancillary qubits in register B , which is the only nontrivial case among all the registers. The number of ancillary qubits in register B is $\sum_{i=\frac{k}{2}}^{n-\frac{k}{2}} \left(\left(\log \binom{\frac{i}{2}}{k} + \log \binom{n-i}{\frac{k}{2}} \right) \right)$. Actually, we have made a stronger estimation in Equation 21, so the number of ancillary qubits in register B is also upper bounded by $O(\binom{n}{k})$, which completes the proof. \square

7 Classical Complexity for Parameter Computation

This section analyzes the classical computational complexity of all the algorithms mentioned above. It is obvious that all the algorithms use quantum gates with parameters (R_y gates) in the Unary Encoding stage. To determine these parameters, we need to calculate the sum of the squares of two adjacent input parameters, and the two input parameters will no longer be used in rest of the circuits. Hence one computation will reduce the number of available parameters by 1. As a result, the classical computational complexity is of the same order as the number of input parameters in each problem.

8 Lower bound

In this section, we will prove the depth and size lower bound of the preparation of HWP states.

Theorem 11 (*Restatement of Theorem 5*) *When using single- and double-qubit gates, almost all the HWP states with parameters n and k need to be prepared in $\Omega(\log \binom{n}{k})$ -depth and $\Omega(\binom{n}{k})$ -size, regardless of the number of ancillary qubits.*

Proof. We first consider depth complexity. For a circuit C with n working qubits and l ancillary qubits, we suppose it has a depth of D to prepare the objective $|\psi\rangle$.

Next, we define a new *directed* graph $G' = \{V', E'\}$. V' , the vertex set of G' , can be divided into $D + 1$ layers, denoted as $v'_{i,j}$ ($i \in [n + l], j \in [D + 1]$), representing the current state. Each layer contains $n + l$ vertices, corresponding to all working and ancillary qubits. As a result, $|V'| = (D + 1)(n + l)$. Edges only appear between two vertices in adjacent layers. The starting (ending) vertex of an edge is always the vertex in the previous (latter) layer. $v'_{i,k}$ in the k^{th} layer and $v'_{j,k+1}$ in the $(k + 1)^{th}$ layer are adjacent if and only if q_i and q_j join the same gate in the k^{th} layer of the circuit. Note that if some q_i does not change in the k^{th} layer, it means there is an identity gate on q_i in the k^{th} layer, so $v'_{i,k}$ in the k^{th} layer and $v'_{i,k+1}$ in the $(k + 1)^{th}$ layer must be adjacent. Obviously, a single-qubit gate in the circuit will generate 1 edge in the circuit, while a double-qubit gate will generate 4 edges. Figure 12 shows a simple circuit and its corresponding directed graph.



Figure 12: A simple quantum circuit and its corresponding directed graph. The red lines shows the light cone of q_3 .

Here we define the light cone of G' . The light cone of G' is a subset of V' . A vertex v' belongs to the light cone if and only if there exists a directed path that starts from v' and ends in one of the working vertices in the last layer, that is some v'_i in the $(D + 1)^{th}$ layer, $i \in \{1, 2, \dots, n\}$. It is not hard to see that only gates within the light cone contribute to the generation of $|\psi\rangle$. Thus, we can simply ignore the gates outside the cone! (The effect of the removal is that the final state may change into $|\psi\rangle |\phi\rangle$ for some $|\phi\rangle$ different from $|0\rangle^{\otimes l}$.)

Actually, any vertex v'_i in the $(k + 1)^{th}$ layer can be the end vertex of at most two directed edges. This leads to the fact that the light cone will contain at most $O(n \cdot 2^D)$ vertices. As each gate can be specified by $O(1)$ parameters, the circuit (after deleting all the gates outside the light cone) can generate at most $O(n \cdot 2^D)$ parameters.

Since an HWP state is characterized by $\binom{n}{k}$ coefficients, the set of all such states with fixed n and k constitutes a $\binom{n}{k}$ -dimensional vector space. If $D \leq \frac{1}{2} \log \binom{n}{k}$, the number of parameters generated by the D -depth circuit C will be $o(\binom{n}{k})$. When the light cone contains $o(\binom{n}{k})$ parameters, the set of HWP states implementable by any circuit sharing C 's structure will be contained within a measure-zero set of the vector space. And there are only finitely distinct circuit structures at depth D , thus the collection of all HWP states that can be prepared within depth D equals the union of finitely many measure-zero sets, which is still measure-zero. Consequently, almost all of the HWP state with parameters n and k can not be prepared by a circuit of depth $\frac{1}{2} \log \binom{n}{k}$.

Next, we consider size complexity, and this is easier. On the one hand, since each single- or

double-qubit gate can be specified by $O(1)$ parameters, the preparation circuit with size S has at most $O(S)$ parameters. On the other hand, an HWP state has $\binom{n}{k}$ coefficients. Similar to the depth analysis, to generate the HWP state successfully, the number of parameters in the circuit must be no less than that of coefficients in the HWP state. Thus, almost all the HWP states with parameters n and k need to be prepared in $\Omega(\binom{n}{k})$ -size. \square

Theorem 12 (Restatement of Theorem 6) *When using single- and double-qubit gates, for almost all the graphs G , the circuit for preparing $|\psi_G\rangle$ needs $\Omega(\log n)$ -depth and $\Omega(m)$ -size, regardless of the number of ancillary qubits.*

Proof. This follows the previous theorem by setting $k = 2$. \square

References

- [Cil+18] Carlo Ciliberto et al. “Quantum machine learning: a classical perspective”. In: *Proceedings of the Royal Society A: Mathematical, Physical and Engineering Sciences* 474.2209 (2018), p. 20170551.
- [SSP15] Maria Schuld, Ilya Sinayskiy, and Francesco Petruccione. “An introduction to quantum machine learning”. In: *Contemporary Physics* 56.2 (2015), pp. 172–185.
- [Bia+17] Jacob Biamonte et al. “Quantum machine learning”. In: *Nature* 549.7671 (2017), pp. 195–202.
- [Ber+15] Dominic W Berry et al. “Simulating Hamiltonian dynamics with a truncated Taylor series”. In: *Physical review letters* 114.9 (2015), p. 090502.
- [LC17] Guang Hao Low and Isaac L Chuang. “Optimal Hamiltonian simulation by quantum signal processing”. In: *Physical review letters* 118.1 (2017), p. 010501.
- [LC19] Guang Hao Low and Isaac L Chuang. “Hamiltonian simulation by qubitization”. In: *Quantum* 3 (2019), p. 163.
- [Yan+18] Yuguang Yang et al. “Quantum network communication: a discrete-time quantum-walk approach”. In: *Science China Information Sciences* 61 (2018), pp. 1–10.
- [Su+20] Xiaolong Su et al. “Quantum network based on non-classical light”. In: *Science China Information Sciences* 63 (2020), pp. 1–12.
- [Dür+06] Christoph Dürr et al. “Quantum query complexity of some graph problems”. In: *SIAM Journal on Computing* 35.6 (2006), pp. 1310–1328.
- [MSS07] Frédéric Magniez, Miklos Santha, and Mario Szegedy. “Quantum algorithms for the triangle problem”. In: *SIAM Journal on Computing* 37.2 (2007), pp. 413–424.
- [SŠ21] S Skoupý and M Štefaňák. “Quantum-walk-based state-transfer algorithms on the complete m-partite graph”. In: *Physical Review A* 103.4 (2021), p. 042222.

[Ber+05] Ville Bergholm et al. “Quantum circuits with uniformly controlled one-qubit gates”. In: *Physical Review A* 71.5 (2005), p. 052330.

[PB11] Martin Plesch and Časlav Brukner. “Quantum-state preparation with universal gate decompositions”. In: *Physical Review A* 83.3 (2011), p. 032302.

[Sun+23] Xiaoming Sun et al. “Asymptotically optimal circuit depth for quantum state preparation and general unitary synthesis”. In: *IEEE Transactions on Computer-Aided Design of Integrated Circuits and Systems* (2023).

[YZ23] Pei Yuan and Shengyu Zhang. “Optimal (controlled) quantum state preparation and improved unitary synthesis by quantum circuits with any number of ancillary qubits”. In: *Quantum* 7 (2023), p. 956.

[DVC00] Wolfgang Dür, Guifre Vidal, and J Ignacio Cirac. “Three qubits can be entangled in two inequivalent ways”. In: *Physical Review A* 62.6 (2000), p. 062314.

[Gre+90] Daniel M Greenberger et al. “Bell’s theorem without inequalities”. In: *American Journal of Physics* 58.12 (1990), pp. 1131–1143.

[Cot+19] William Cottrell et al. “How to build the thermofield double state”. In: *Journal of High Energy Physics* 2019.2 (2019), pp. 1–43.

[Van+21] John S Van Dyke et al. “Preparing Bethe ansatz eigenstates on a quantum computer”. In: *PRX Quantum* 2.4 (2021), p. 040329.

[GH21] Niels Gleinig and Torsten Hoefer. “An efficient algorithm for sparse quantum state preparation”. In: *2021 58th ACM/IEEE Design Automation Conference (DAC)*. IEEE. 2021, pp. 433–438.

[LL25] Lvzhou Li and Jingquan Luo. “Nearly optimal circuit size for sparse quantum state preparation”. In: *52nd International Colloquium on Automata, Languages, and Programming (ICALP 2025)*. Schloss Dagstuhl–Leibniz-Zentrum für Informatik. 2025, pp. 113–1.

[LLL25] Jingquan Luo, Guanzhong Li, and Lvzhou Li. “Space-time tradeoff for sparse quantum state preparation”. In: *arXiv preprint arXiv:2506.16964* (2025).

[Dic54] Robert H Dicke. “Coherence in spontaneous radiation processes”. In: *Physical review* 93.1 (1954), p. 99.

[ÖSI07] Sahin K Özdemir, Junichi Shimamura, and Nobuyuki Imoto. “A necessary and sufficient condition to play games in quantum mechanical settings”. In: *New Journal of Physics* 9.2 (2007), p. 43.

[FA02] Adrian P Flitney and Derek Abbott. “An introduction to quantum game theory”. In: *Fluctuation and Noise Letters* 2.04 (2002), R175–R187.

[Pre+09] Robert Prevedel et al. “Experimental realization of Dicke states of up to six qubits for multiparty quantum networking”. In: *Physical review letters* 103.2 (2009), p. 020503.

[BE22] Andreas Bärtschi and Stephan Eidenbenz. “Short-depth circuits for dicke state preparation”. In: *2022 IEEE International Conference on Quantum Computing and Engineering (QCE)*. IEEE. 2022, pp. 87–96.

[YZ25] Pei Yuan and Shengyu Zhang. “Depth-Efficient Quantum Circuit Synthesis for Deterministic Dicke State Preparation”. In: *arXiv preprint arXiv:2505.15413* (2025).

[MYD22] Fereshte Mozafari, Yuxiang Yang, and Giovanni De Micheli. “Efficient preparation of cyclic quantum states”. In: *2022 27th Asia and South Pacific Design Automation Conference (ASP-DAC)*. IEEE. 2022, pp. 460–465.

[Mon+23] Léo Monbroussou et al. “Trainability and expressivity of hamming-weight preserving quantum circuits for machine learning”. In: *arXiv preprint arXiv:2309.15547* (2023).

[Cao+23] Sirui Cao et al. “Generation of genuine entanglement up to 51 superconducting qubits”. In: *Nature* 619.7971 (2023), pp. 738–742.

[MTS24] Rui Mao, Guojing Tian, and Xiaoming Sun. “Towards Optimal Circuit Size for Quantum Sparse State Preparation”. In: *arXiv preprint arXiv:2404.05147* (2024).

[Jia+20] Jiaqing Jiang et al. “Optimal space-depth trade-off of CNOT circuits in quantum logic synthesis”. In: *Proceedings of the Fourteenth Annual ACM-SIAM Symposium on Discrete Algorithms*. SIAM. 2020, pp. 213–229.

[Joh+21] Sonika Johri et al. “Nearest centroid classification on a trapped ion quantum computer”. In: *npj Quantum Information* 7.1 (2021), p. 122.

[Gid] Craig Gidney. <https://algassert.com/circuits/2015/06/05/Constructing-Large-Controlled-Not.html>.

[NC10] Michael A Nielsen and Isaac L Chuang. *Quantum computation and quantum information*. Cambridge university press, 2010.

[ZNS25] Wei Zi, Junhong Nie, and Xiaoming Sun. “Shallow quantum circuit implementation of symmetric functions with limited ancillary qubits”. In: *IEEE Transactions on Computer-Aided Design of Integrated Circuits and Systems* (2025).

[Die24] Reinhard Diestel. *Graph theory*. Springer (print edition); Reinhard Diestel (eBooks), 2024.

[Die17] Reinhard Diestel. “Extremal Graph Theory”. In: *Graph Theory*. Berlin, Heidelberg: Springer Berlin Heidelberg, 2017, pp. 173–207. ISBN: 978-3-662-53622-3. DOI: 10.1007/978-3-662-53622-3_7.